Report 2005

Erstes DELTA
User-Meeting

Dortmund
30. November 2005

Vorwort

DELTA, das Synchrotron mit dem besonderen Etwas, hat ab heute eine neue Einrichtung:

Das DELTA User-Meeting.

So erstatten wir zum ersten Mal Bericht, erheben aber keinen Anspruch auf Vollständigkeit. Aus User Sicht erhoffe ich mir aus diesem ersten Treffen, in dem wir unsere Ergebnisse der vergangenen „Jahres-Strahlzeit“ nebst unseren Wünschen dem Direktorium präsentieren, gewisse Synergieeffekte für die Zukunft.

Unsere Wünsche werden bestimmt während des Treffens geäußert werden und sind dem Protokoll zu entnehmen. Persönlich wünsche ich uns an erster Stelle weiterhin einen kontinuierlichen Betrieb von DELTA, da er die Grundlage zur Realisierung vieler Forschungsvorhaben ist.

Dem Direktorium und der DELTA-Mannschaft sei hier gedankt. Ich hoffe sehr, Sie alle finden ihre Bemühungen „Strahl erster Güte“ dem Nutzer zur Verfügung zu stellen in den Ergebnissen der nachfolgenden Berichte widergespiegelt.

DELTA ist klein aber fein! Und gerade deshalb schaut die ganze Fachwelt auf die Qualität unserer Arbeit.

Alex von Bohlen

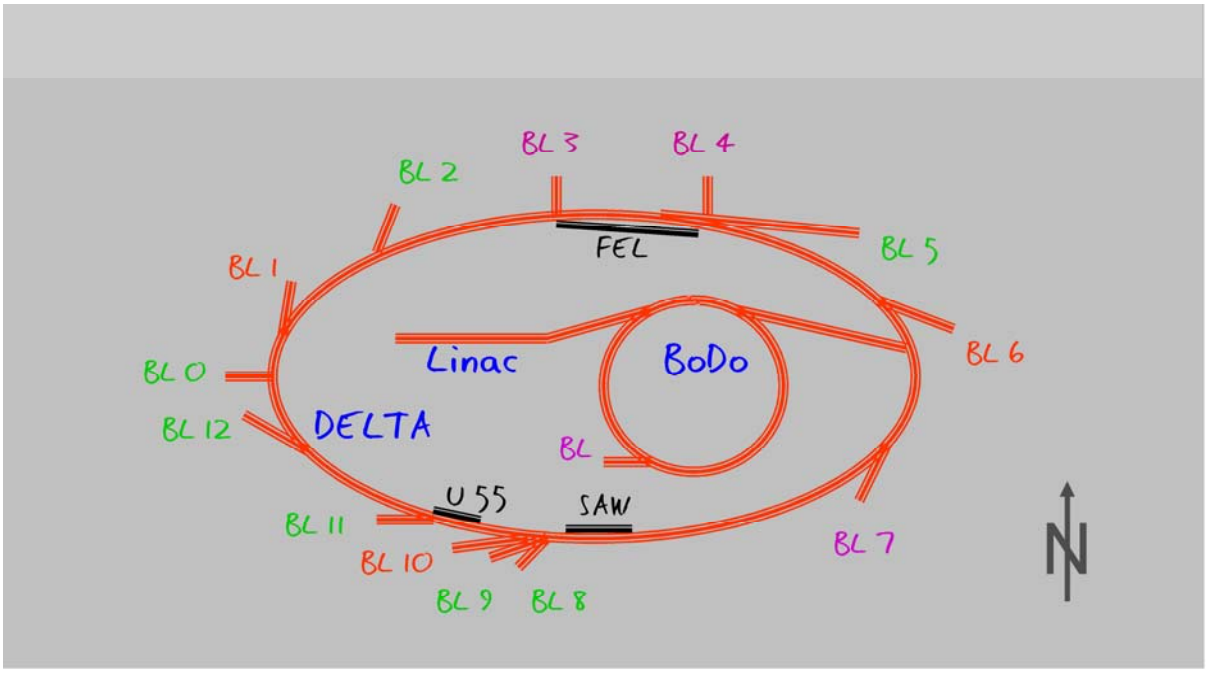

In grün markierte Strahllinien stehen dem Benutzer zur Verfügung

Aufbau der DELTA Infrarot-Beamline

K. Wille[1], T. Weis[1], B. Hippert[1], N. Nedelchev[2], E.H. Korte[2]

[1] DELTA, Universität Dortmund, 44221 Dortmund
[2] ISAS - Institute for Analytical Sciences, Bunsen-Kirchhoffstr. 11, 44139 Dortmund

Die Leistungsfähigkeit moderner Infrarot-Spektrometer lässt leicht vergessen, dass nur der langwellige Ausläufer der Schwarzkörper-Strahlungsverteilung genutzt wird. Üblicherweise wird die Strahlung einer thermischen Quelle von einigen 10 mm² auf eine etwa gleichgroße Fläche am Ort der Probe gebündelt. Einer stärkeren Fokussierung ohne den ausgenutzten Raumwinkel an der Quelle oder deren erfasste emittierende Fläche (konstanter Lichtleitwert) zu reduzieren sind enge Grenzen gesetzt. Dies ist insbesondere für die Mikroskopie nachteilig.

Synchrotron-Strahlung bietet eine dagegen kleine Quellfläche und durch die Vorwärtsrichtung der Abstrahlung günstigere Bedingungen für kleine Proben. So wurde bei einem direkten Vergleich an der IRIS-Beamline bei BESSY in Berlin für Proben unter 1 mm^2 Fläche ein um mindestens den Faktor 20 besseres Signal-Rausch-Verhältnis als bei Verwendung einer thermischen Quelle gefunden [1]. Dieser Faktor steht in der Praxis tatsächlich zur Verfügung, Verluste z.B. durch die Transferoptik und das den UHV-Teil abschließende Fenster sind berücksichtigt.

Gegenüber anderen Spektralbereichen müssen im Infrarot-Bereich einige Besonderheiten berücksichtigt werden:
- die natürliche Divergenz in der Vertikalen (senkrecht zur Ringebene) ist deutlich größer als im Kurzwelligen, dies wird häufig genutzt um die harte Strahlung in der Ringebene z.B. durch einen Absorber zu eliminieren;
- auch horizontal muss ein größerer Sektor des Strahlungsfächers erfasst werden (z.B. 80 mrad) um ausreichend Strahlungsleistung zu extrahieren,
- wegen der Divergenz in beiden Richtungen ist eine abbildende Strahlführung vom Speicherring bis zum Spektrometer außerhalb der Schutzmauer vorteilhaft, da sich so der Bündeldurchmesser limitieren lässt,
- wegen der spektralen Breite des Infrarot-Bereiches werden Spiegel zur Bündelführung eingesetzt, Hohlspiegel führen aber bei achsennaher Verwendung zu einem sperrigen, langwegigen Aufbau, ansonsten zu Abbildungsfehlern und damit potentiell zu Verlusten.

Für die Infrarot-Beamline bei DELTA wurden neue Wege beschritten. Der erste Spiegel wurde dicht am gespeicherten Elektronenstrahl in einem Ablenkmagneten positioniert, er reflektiert Strahlung in radialer Richtung zum Kreisbogen der Trajektorie. Wegen der Nähe zum Entstehungsort der Strahlung erfasst er trotz der vergleichsweise geringen Abmessungen von ca. 35 mm x 52 mm einen beträchtlichen Raumwinkel. Der gekühlte Spiegelkörper ist aus Sauerstoff-freiem Kupfer gefertigt, so dass im Wesentlichen Infrarot-Strahlung reflektiert wird. Der

Spiegel kann soweit aus der Nachbarschaft des Elektronenstrahls zurück gezogen werden, dass seine Rückseite die Auslassöffnung dem Kammerprofil entsprechend verschließt.

Der Spiegel ist einachsig zirkular gekrümmt und bewirkt eine gute Kollimation in der horizontalen Ebene. Die bisherigen Beobachtungen lassen erwarten, dass für die Phase der grundlegenden Untersuchungen keine weiteren abbildenden Elemente für den Strahlungstransfer bis außerhalb der Schutzmauer notwendig sind. Die Kammer ist derzeit mit einem Quarzfenster abgeschlossen, das zwar den mittleren Infrarot-Bereich blockiert, aber die Beobachtung im nahen Infrarot erlaubt, wo die vertikale Divergenz noch akzeptiert werden kann. Das Strahlführungsrohr soll evakuierbar oder Stickstoff-spülbar ausgelegt werden. Eine Kammer außerhalb der Mauer ist u.a. aus Strahlenschutzgründen für eine 90°-Ablenkung vorgesehen.

Ein planer Spiegel in dieser Kammer dient der Messung der Intensitäts- und Polarisationsverteilung über den Strahlquerschnitt; dafür steht ein speziell entwickeltes Messinstrument [2] zur Verfügung. Durch Wechsel zu einem fokussierenden Spiegel können kommerzielle Spektrometer mit Mikroskop oder anderer Probenoptik angekoppelt werden. Bei einem späteren Ausbau der Transferoptik sollen zusätzliche Spiegel die Justage und Stabilisierung des Strahls und Zwischenabbildungen kleinere Fensterflächen erlauben, so dass deren Material optimal primär für das jeweilige Experiment gewählt werden kann.

Parallel zum ersten Aufbau der Beamline und ihrer Charakterisierung wird das Interferometer eines kommerziellen Spektrometers für Polarisationsmodulation umgebaut und seine Vorteile für die Infrarot-Ellipsometrie getestet. Ziel ist es, bei ellipsometrischen Messungen systematische Fehler zu vermeiden, die bei Verwendung des bisher notwendigen Retarders (Phasenschiebers) nicht auszuschließen sind und bei wenig ausgeprägten Analysensignalen, wie sie beispielsweise bei kleinen Probenflächen mit molekularen Monolagen vorliegen, eine gravierenden Einfluss haben können.

[1] M. Gensch, K. Hinrichs, A. Röseler, E.H. Korte, U. Schade;
Analytical and Bioanalytical Chemistry 376 (2003) 626-630

[2] U. Schade, A. Röseler, E.H. Korte, M. Scheer, W.B. Peatman;
Nuclear Instruments and Methods in Physical Research A, 455 (2000) 476-488

New developments in X-ray Spectroscopy
- The ISAS Synchrotron Microprobe at DELTA

Alex von Bohlen
Institute for Analytical Science ISAS-Dortmund
Bunsen-Kirchhoff-Str. 11
44139 Dortmund

In recent years several important developments in the field of analytical techniques using X-rays have been achieved. Synchrotron radiation has been discovered to be an excellent excitation source for X-ray fluorescence spectrometry. Detailed studies have been conducted to establish the advantages of using synchrotron radiation for X-ray fluorescence spectrometry. However, nearly all published papers in this area of applications have dealt with energy dispersive X-ray fluorescence spectrometry.

Since 2004 the ISAS operates a beamline at the synchrotron facility DELTA at University of Dortmund. An official contract between ISAS and DELTA has been signed before. Since this time synchrotron radiation (SR), an excellent excitation source for X-ray fluorescence spectrometry (XRF), is available at the "ISAS-Line".

Among others, the high brilliance of the source in contrast to the conventional X-ray tube, the strong polarization of the radiation and the low divergence of the beam can be applied to XRF offering several advantages for spectroscopy. These outstanding features encouraged us to develop and operate a SR induced X-ray micro fluorescence probe connected to a wavelength dispersive spectrometer (SR-WDXRF). A relevant characteristic of such a device, namely, good lateral resolution at high spectral resolution can be applied for single spot-, line-scan and area map analyses of a variety of objects.

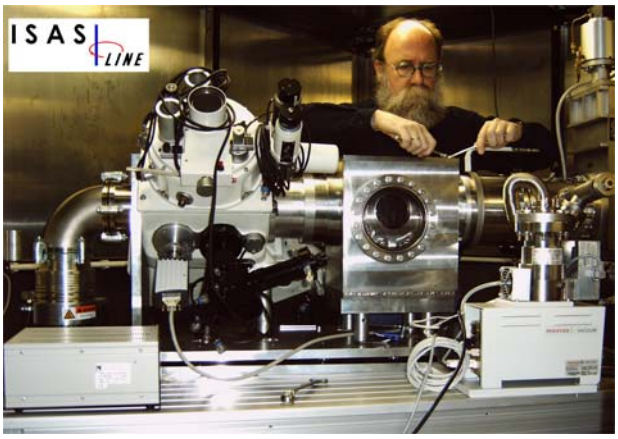

Figure 1. ISAS prototype spectrometer for synchrotron radiation induced wavelength X-ray fluorescence spectrometry.

Our prototype contains as an essential part of the body of a scanning electron microprobe containing two focussing double crystal spectrometers (Fig. 1). It was adapted and attached to the ISAS-Line. Additionally, a special vacuum chamber containing two remote controlled stages was designed and constructed. One of them is supporting the X-ray optics and the other a slit system. With the aid of different X-ray optics – mono-capillaries, poly-capillaries and arrays of refractive devices – synchrotron radiation can be focused to produce a probe smaller than15 μm in diameter.

The SR-WDXRF micro fluorescence spectrometer operated under vacuum conditions will be useful for the detection of light elements by their fluorescence K-lines (e.g. carbon, oxygen,

nitrogen, fluorine, potassium, magnesium, aluminium, etc., cf. Fig. 2.). Further elements are also accessible with high lateral resolution of some micrometers. They can also be detected with good spectral resolution of some eV by their respective L- or M-lines.

The method offers ideal conditions for the analysis of microtome sections of non-conducting materials. This potential will be applied in a common project of monitoring the element distribution in cancerous and normal human tissue in collaboration with the Department of Physics, University Lisbon. Other applications of the method to the element characterization in samples of bio-medical origin are planed.

Another promising application of SR-WDXRF exploiting the excellent spectral resolution at high intensity of the primary beam concerns the speciation of element compounds. Shifts of some selected X-ray transition lines can be used for a quantitative evaluation of species. Interesting measurements for the species analysis of sulphur, of aluminium, chromium, manganese and others are expected for material analysis.

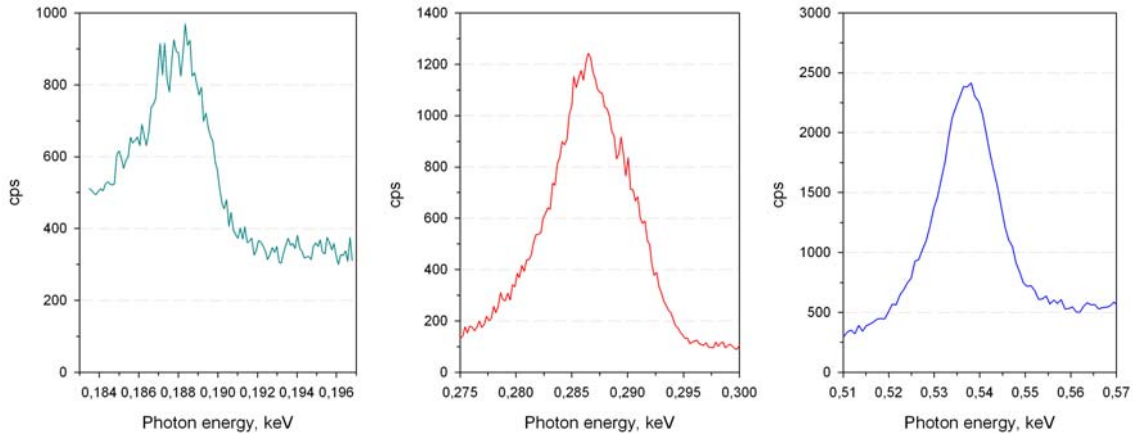

Fig. 2. Spectra recorded by SR-WDXRF representing the Kα-line of boron, carbon, and oxygen, respectively. Data obtained at DELTA BL 2, excitation white beam, analyzer crystal STE (lead stearate).

Publications

A. von Bohlen, R. Hergenröder, C. Sternemann, M. Paulus, M. Radtke, H. Riesemeier. Wavelength dispersive synchrotron microprobe used for material analysis. Instrumentation Science & Technology, 33 (2005) 137 – 150.

DELTA User Meeting 2005

Report -Beamline 5

Project

"Spin-polarised photoemission spectroscopy at the Mg_xO_{1-x} / Fe interface"

Participants:
Frank Matthes, Martina Müller, Stefan Cramm, Lutz Baumgarten, Claus M. Schneider

Institute of Solid State Research (IFF), Research Centre Jülich, 52425 Jülich, Germany
Contact: F.Matthes@fz-juelich.de

Motivation
This research project is focused on the electronic band structure at the interface of magnetic tunnel junctions (MTJ). MTJ's have attracted large interest because they can be used to build up sensors for reading heads in hard discs, non-volatile magnetic random access memories (MRAM) or programmable logic devices.
MTJ's may be formed by two magnetic electrodes that are separated by an insulating material that is thin enough to allow a tunnel process. The decisive property of MTJ's is that the tunnel current may depend strongly on the relative magnetization direction of the two electrodes. Changing from parallel to antiparallel alignment, the tunnel resistance may increase by more than 220% at room temperature[1].
A prominent representative of MJT is the single crystalline trilayer system: Fe/MgO/Fe. It serves as a model system for theoretical calculations of the spin-dependent tunnel current and allows to study the influence of the symmetry depending matching of the wave functions involved in the tunnel process. Important for the modelling is the knowledge of the spin-dependent electronic band structure of the two electrodes and its possible changes introduced by the insulation barrier. Up to know, the microscopic properties at the interface is still not fully understood. Using spin-resolved valence band photoemission spectroscopy, we found a spin-dependent attenuation of photo electrons excited from the minority Δ_5 band of iron upon the deposition of MgO[2]. Because the origin of this effect is still under discussion, we have extended our measurements to the interface to iron and MgO where MgO is partially over- or under oxidized.

Experimental setup
Our experimental setup consists of two UHV chambers, one dedicated to sample preparation and one to perform spin- and angle-resolved photoemission spectroscopy. A linear transfer arm allows the sample exchange between the chambers within one minute. Thus the photoemission experiments can start immediately after sample preparation, avoiding any adsorption of resident gas particles onto the clean sample surface.

The spectrometer system houses an electrostatic cylindrical sector analyser (CSA) equipped with an optimized lens transfer system to achieve highest transmission. The CSA features a 90° deflection, which permits the electron spin analyser to measure simultaneously one in-plane and the out-of-plane component of the surface magnetization. The spin analysis is achieved by spin-dependent elastic scattering at a W(100) surface at a fixed kinetic energy of 104,5 eV [3]. Using the electron intensity of two opposite diffraction spots, we can determine the spin asymmetry of one component. The maximum achievable energy resolution with acceptable count rates (measurement times) is 50 meV (full width half maximum). The angular acceptance angle is ± 6°. To exclude the influence of detector asymmetries, we repeat our measurements with two opposite magnetization directions.

The preparation chamber is equipped with a sample manipulator having two translation and two rotation axes. Cooling and heating options allow substrate preparation and a controlled manipulation of the film growth conditions. The minimum sample temperature is 150 K. Momentary equipped with

an indirect heating option, we can achieve sample temperatures of up to 870 K. Higher temperatures can be reached by electron beam assisted heating.
For the in-situ characterization of the chemical composition we apply Auger electron spectroscopy. The structural properties of the grown thin films can be determined by low energy electron diffraction. The thickness of films growing in a Franck–van der Merwe mode can be precisely measured in fractions of monolayers by medium energy electron diffraction. Otherwise, we estimate the thickness by the attenuation of the element specific Auger electron intensity signals. The film growth is achieved by electron assisted evaporation from rod materials or from crucibles. Our chamber is equipped with an optical set-up that allows to measure in-situ the magneto optical Kerr effect in longitudinal and polar geometry.
Samples and substrates can be introduced via a load-lock system without breaking the UHV of the preparation chamber.

Experiments and results

The sample preparation and the photoemission measurements have been performed under ultrahigh vacuum conditions. The base pressure is below $2*10^{-10}$mbar. Ten monolayer thin Fe films were grown on GaAs(100) substrates. Substrate preparation and epitaxial growth conditions are described elsewhere[2]. In-situ magneto-optical Kerr-effect measurements confirmed a ferromagnetic ordering at room temperature with the easy axis oriented along the [110] direction. To grow Mg_xO_{1-x} films with different oxygen content, we evaporated pure Mg from a crucible and simultaneously offered molecular oxygen with different oxygen partial pressures.

Our beam line offers linear polarized light with the electric field vector lying in the plane defined by the k-vector of the incident beam and the k-vector of the detected photoelectrons. The incident light made an angle of 45° with the surface normal. In this geometry we have components of the electric field vector in-plane along the [110] direction and perpendicular to the sample surface. The photoelectrons were detected along the surface normal. Following the dipole selection rules such a geometry allows direct transitions from initial states with Δ_1 and Δ_5 spatial symmetry into final states with Δ_1 spatial symmetry.

Using a fixed photon energy of 34,2 eV for the pure iron films, we have excited direct dipole transitions from the majority Δ_1 symmetry band located 0,9 eV and from the minority Δ_5 symmetry located at 0,4 eV below the Fermi level. Furthermore, we could identify direct transitions from the lower minority Δ_1 symmetry band located 3.4 eV below the Fermi level.

To study the influence of Mg_xO_{1-x} on the electronic band structure of the iron films, we started first with increasing coverage of nominal pure Mg. Measuring the shape and energy position of the 2p Mg level, we found out that we can not avoid a partial oxidation of the deposited Mg. The minimum oxidation rate of the Mg was 30 %. Upon Mg coverage up to nominal 1,5 monolayers, our photoemission measurements revealed a clear tendency of the measured spin polarization to larger positive values (increase about 50%). This was measured for both direct transitions from the two iron bands located 0,9 eV and 0,4 eV below the Fermi level.

In a second step, we exposed the iron films to molecular oxygen with increasing exposure doses of 0,7 L, 4,5 L and 8,2 L. The hereby introduced changes in the spin-resolved photoemission spectra were not as large as in the case for Mg and they didn't show the same tendency for the above mentioned direct transitions from iron. Another remarkable difference compared to the coverage with Mg was a clear suppression of the transition from the lower lying minority Δ_1 symmetry band, located at 3,4 eV below Fermi level. It happened already after the exposure to 0,7 L molecular oxygen.

References

1. Stuart S.P. Parkin, C. Kaiser, A. Panchula, P. M. Rice, B. Hughes, M. Samant and S.-H. Yang, Nature Materials **3**(2004) p. 862, S. Yuasa, T. Nagahama, A.Fukushima, Y. Suzuki and K. Ando, Nature Materials **3**(2004) p. 868

2. F. Matthes, L.-N. Tong, C.M. Schneider, J. Applied Physics **95**(2004) p. 7240

3. J. Kirschner and R. Feder: Phys. Rev. Lett. **42**, (1979) p.1008

The Materials Science Beamline BL8 at DELTA

R. Wagner, D. Lützenkirchen-Hecht and R. Frahm
Fachbereich C / Physik, Bergische Universität Wuppertal, Gaußstraße 20, D-42097 Wuppertal

Electron storage rings with insertion devices create intense, brilliant X-ray beams which are well suited for many experimental applications in materials science. In our case, the Superconducting Asymmetric Wiggler (SAW) at the DELTA storage ring operating at 1.5 GeV electron energy provides a continuous spectrum of circularly polarized photons with a high intensity between 1 keV and 30 keV, which is ideally suited for X-ray absorption experiments (XAFS). The radiation is emitted into a horizontal fan of ± 25 mrad, so that three beamlines can be operated in parallel. The central beamline is operated by the University of Dortmund. At the two remaining beam ports we are currently installing two new materials science beamlines. Here we focus on the general purpose beamline BL 8 which is especially designed for the requirements of all XAFS methods as well as of XRD-measurements with the possibility of focussing a wide spectral range.


Diffractometer BL8

The front end mainly consists of an absorber mask which defines the initial beam size and two monitors for the measurement of the position and the angle of the photon beam. Besides components for radiation protection, vacuum control, slit systems for beam definition and several devices for additional beam characterization, the main X-ray optical components are the double crystal monochromator (DCM) and the Rh-coated mirror systems. The first collimating (plane) mirror is responsible for vertical focussing. The elimination of the beam divergence also increases the energy resolution of the DCM, which has a fixed beam offset. The first crystal of the DCM is equipped with a special crystal bender to compensate the deformation due to the thermal load produced by the white beam of the wiggler.

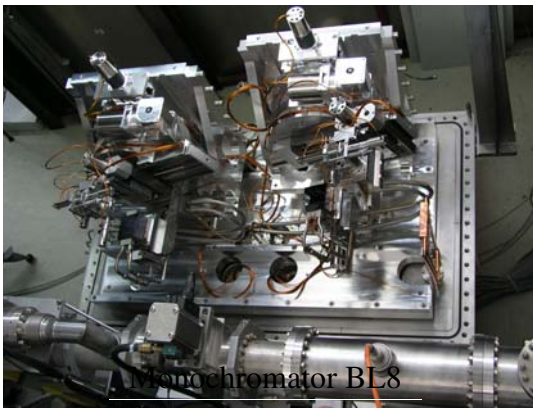
Monochromator BL8

To cover the whole energy range, the DCM contains three different crystal pairs that can be changed by remote control without breaking the vacuum. While YB_{66} crystals are used for the 1-2 keV energy region, Si(111) and Si(311) are employed for the ranges 2-12 keV and 8-30 keV, respectively. Mirrored beams will be available in the energy range between 1 keV and 15 keV. In this case, the bendable second (toroidal) mirror focuses the radiation onto the specimen. Horizontal focussing at higher energies will be obtained by a Si(311) crystal which is equipped with a sagittal bending mechanism. The expected beam size on the sample is less than 0.5 mm^2. Harmonic rejection will usually be achieved by detuning the crystals with respect to each other by piezo tilt stages, and an additional double mirror device with an adjustable energy cut-off from 2 to 5 keV is used for harmonic rejection in the 1-2 keV photon energy range.

Planned scientific projects are e.g. structural analysis of thin films, in situ characterization of reactively sputtered films, phase transitions in thin films and multilayers, and investigations of catalytic reactions. Currently, the beamline is under commissioning, and first used beam is expected at the end of 2005.

Report of x-ray diffraction measurements at DELTA-beamline for studying the crystallographic orientation of chitin and calcite in lobster and crab shells (08-12 Nov. 2004).

Ali Al-Sawalmih[1)], Dierk Raabe[2)]
[1)] Max-Planck-Institute for Eisenforschung-Düsseldorf, Max-Planck-Str. 1, 40237 Düsseldorf, sawalmih@mpie.de
[2)] Project leader, Max-Planck-Institute for Eisenforschung-Düsseldorf, Max-Planck-Str. 1, 40237 Düsseldorf, raabe@mpie.de

Introduction:

Lobster and crab shells contain chitin fibers associated with crystallites of calcite (not necessarily pure calcite). In this study, powder diffraction and methods of X-ray texture analysis were used to determine the diffraction profile of lobster and crab powder, and texture strength of calcite in the crab shell, respectively. A synchrotron X-ray beam (13 KeV) was employed. Texture measurements in the beamtime were devoted for the calcite texture of the (104) reflection, because crab shell sample revealed strong calcite reflections, comparing to lobster, which contains amorphous calcium carbonate as a compensation ratio with calcite. The synchrotron X-ray powder diffraction results measured at beamline BL9 of DELTA were consistent with the ones carried out at ANKA-Karlsruhe using PX-beamline.

Results:

Parts of lobster and crab shells were milled at the physics laboratory-University of Dortmund and filled in quartz capillaries of 500 µm diameter. The powder capillary was mounted on a goniometer head in a six circle goniometer. Diffraction intensities were recorded with a NaI point detector. The detector was scanning the intensities in the range of the expected reflections. Exposure time ranged from 10 and 20 seconds. The data were processed with the ORIGIN software. Figure 1 shows the diffraction profile of lobster shell powder, crab shell powder, and empty capillary as a background.

Fig. 1

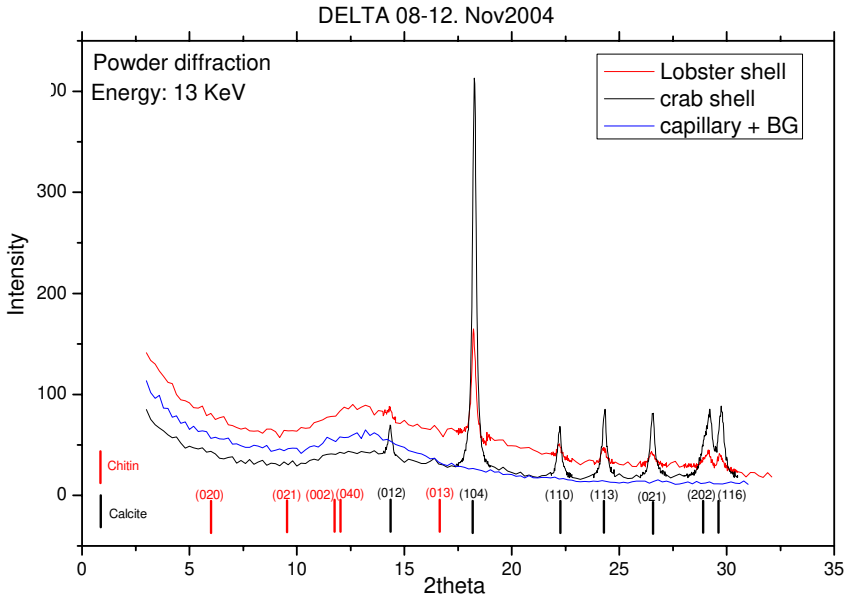

Chitin reflections were not observed, because chitin as a polymer consisting mainly Carbon and Oxygen- is not a strong x-ray scatterers, compared to calcite, which gave a strong reflections. Obviously with an area detector, one can get better intensities for chitin, because it is possible to make a summation of intensity over circular rings corresponding to the diffraction cones, which in turn gives higher intensity and make it observable. The diffraction

spectra measured at ANKA PX-beamline utilizing a CCD detector, as presented in Fig. 2 for comparison, emphasizes the use of area detector for texture measurements.

Fig. 2

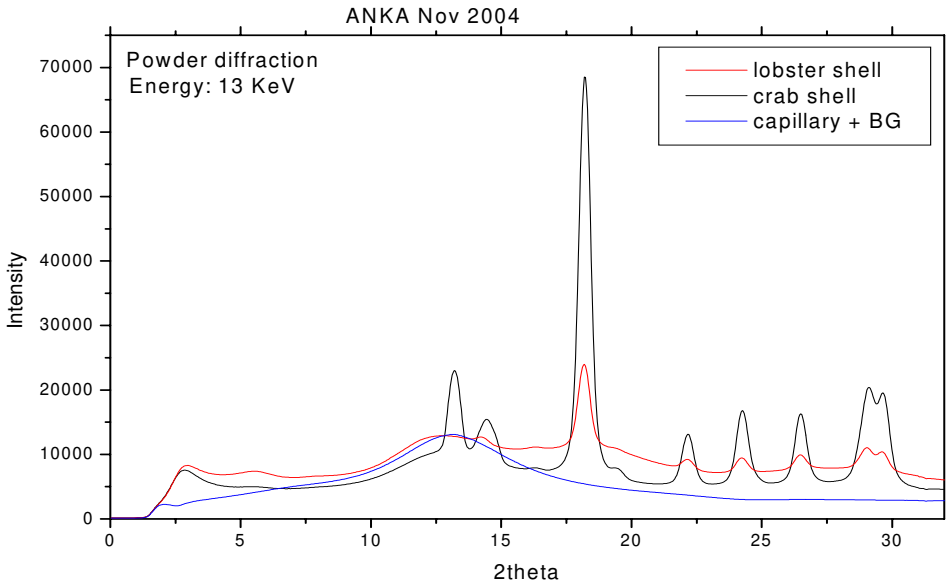

Due to the use of point detector, it was difficult to perform the texture analysis for all samples and for the observed reflections of calcite, so we could only do it for the strongest reflection (104) for one sample.

The output raw data was processed and it was possible to draw a pole figure out of it, which represents the crystallographic orientation of that plane (104) with respect to sample geometry. From this relation and with support of different pole figures for other calcite reflections, we can reveal the texture of calcite in crab shell. Further analysis related to the created pole figure is in progress. We performed a full texture analysis for more than 15 samples, covering calcite and chitin, at ANKA-Karlsruhe which is supported with a CCD camera.

The availability of MAR-detector at beamline BL9 of DELTA will solve the problem resulting from using a point detector for application in texture analysis where is no need for such a high resolution supported by the point detector setup and intensity play the key role. The new MAR setup together with the six circle goniometer will be ideal to perform texture analysis on this kind of biological samples.

Acknowledgement:

I thank Dr. Christian Sternemann for his assistance and support during our beamtime, and his patience and care. Furthermore I would like to thank Mr. Dirk Schemionek- Universität Dortmund, for his help and support in preparing the powder samples.

Measurement of strains stored in NaCl powder containing CuCl nanocrystals

H.-J. Weber,[†] C. Varga-Popa,[†] H.-L. Keller,[‡] M. Schlosser,[‡] M. Paulus,[⋆] and C. Sternemann[⋆]

[†] *Institut für Physik, Universität Dortmund, D-44221 Dortmund, Germany*

[‡] *Fachbereich Chemie, Universität Dortmund, D-44221 Dortmund, Germany and*

[⋆] *Institut für Physik, DELTA, Universität Dortmund, D-44221 Dortmund, Germany*

(Dated: October 26, 2005)

Introduction: Our main interest is the investigation of the forces acting between nanocrystals and a three-dimensional crystalline matrix. In CuCl:NaCl we observed by resonant ultrasound spectroscopy a small elastic hardening by CuCl nanocrystals where the state of CuCl was determined by exciton spectroscopy.[1] The hardening was two orders of magnitude larger than expected from the elastic continuum theory. An even stronger increase of elastic constants was observed by x-ray powder diffraction under hydrostatic pressure p_0 at Hasylab, DESY.[2] In addition, a compression of 2×10^{-3} due to the impact of nanocrystals was obtained for $p_0 = 0$. These results are consistent with a piezoelectric coupling between nanocrystals and matrix and/or with the influence of free elastic surfaces. The latter effect was verified by optical measurements on thin plates.[2]

In a first diffraction experiment at the beam-line BL9(SAW2) of DELTA we have demonstrated that the elastic continuum theory works quantitatively if piezoelectric coupling is absent which is the case for KCN:KI.[3] In the present work we intend to determine the spontaneous strain induced by CuCl nanocrystals in the matrix of CuCl:NaCl without the additional action of external stresses as it had been done before[2].

Experimental: A preliminary measurement has shown the anomalous but interesting result that the line-width FWHM of Bragg reflections was more narrow in the doped material CuCl:NaCl than in pure NaCl which indicated the need for a systematic comparison between both kind of materials. This was done by use of 13 powder samples made from 9 different bulk crystals. The mole fractions of total CuCl x and of crystalline CuCl x_{cr} varied in the ranges $2 \times 10^{-4} < x < 1.9 \times 10^{-3}$ and $0.9 \times 10^{-4} < x_{cr} < 1.27 \times 10^{-3}$. The difference $x - x_{cr}$ is a measure of the Cu^+-ions which occupy statistically the octahedral Na^+-positions of the matrix. The concentration and the state of CuCl was determined by optical absorption measurements in the near UV-range. X-ray diffraction measurements of high resolution were accomplished at the beam-line BL9(SAW2) of DELTA utilizing the 6-circle diffractometer. Most measurements were performed between 19° [(200)-reflection] and 86° [(820)-reflection]. For five samples measurements were performed at several fixed temperatures

between 25°C and 100°C.

For the sake of comparison one sample was prepared of pure KCl and three samples of CuCl:KCl with varying CuCl concentrations in the melt. In all three crystals doping was nearly the same: $x_{cr} \approx 3 \times 10^{-5}$ and $x \approx 1.8 \times 10^{-4}$.

Results: In pure NaCl and in CuCl:NaCl with $x_{cr} < 1.5 \times 10^{-4}$ the FWHM of the Bragg peaks consists of two contributions, a constant one and one that increases with $\tan\Theta$, where Θ denotes the Bragg-angle. Roughly spoken, the constant term is the same in all samples. It is consistent with the estimated resolution of the apparatus. The contribution that increases with the Bragg-angle is assumed to be a measure of the internal strains S_{cd}. As the Bragg-peaks are symmetric, S_{cd} represents a continuous distribution of stored strains with negative and positive values. The lattice parameter decreases linearly with increasing S_{cd}. Extrapolating to $S_{cd} = 0$ yields the reference value a_0. With respect to a_0, all observed data indicate a stored negative strain $|S_I| \approx \frac{1}{3}|S_{cd}|$.

In pure KCl, $S_{cd} = 0$ but $S_{cd} \neq 0$ appears in CuCl:KCl and the lattice parameter is the same in all four materials. This behavior contrasts strongly to that of NaCl.

In CuCl:NaCl with $x_{cr} > 1.5 \times 10^{-4}$, $S_{cd} = 0$. Nevertheless, also in these materials a stored negative strain is observed (it is called S_{II}). S_{II} depends on x_{cr} like an order parameter in a phase transition of first order. The observed value $S_{II} = -3.2 \times 10^{-4}$ is significantly larger than the value expected by theory but it presents only a part of the strain obtained under the action of an hydrostatic pressure.[2]

Final Remarks: The present results support the idea of piezoelectric coupling between CuCl nanocrystals and the NaCl matrix and represent an experimental basis for the development of an interaction model that goes beyond the simple elastic continuum theory. In addition we observed surprisingly strong differences of stored strains due to only small variations of the material which indicate the existence of unusual threshold-conditions.

---

[1] H.-J. Weber, J. Schreuer, and C. Popa-Varga, *Phys. Rev. B*, **69** 235419 (2004).

[2] H.-J. Weber, H.-L. Keller, C. Lathe, and C. Popa-Varga, *J. Appl. Phys.* **98**, 034317 (2005).

[3] H.-J. Weber, H.-L. Keller, M. Paulus, and C. Sternemann, *Phys. Rev. B*, **72**, 045432 (2005).

Investigation of the initial stages of iron aluminide oxidation regarding the crystallisation of Al_2O_3 polytypes

M. Spiegel
'High Temperature Reactions'
Dept. of Interface Chemistry and Surface Engineering
Max-Planck-Institute für Eisenforschung GmbH

MPIE User Report

1. Project

Investigation of the initial stages of iron aluminide oxidation regarding the crystallisation of Al_2O_3 polytypes

2. Introduction

Iron aluminides are potential materials for high temperature application, if a protective α-Al_2O_3 scale is formed on the metal surface. At temperatures below 1000 °C the growth of metastable, less protective Al_2O_3 polymorphs (for example monoclinic θ-Al_2O_3 and cubic γ-Al_2O_3) is reported and assumed to take place during the initial stages of oxidation [1-4]. However, investigations on the inital stages of oxidation often show the formation of a double oxide layer consisting of an outer iron-rich oxide followed by an inner Al_2O_3 layer [5-8]. So far, it is discussed quite controversely which phases are present within this double layer after the inital stages of oxidation. As alumina exists in different modifications and also reacts with iron oxide to form a spinel phase of $FeAl_2O_4$ composition or a $(Fe, Al)_2O_3$ solid solution phase. The aim of the present study is to analyse the oxide layers formed on iron aluminides of different composition especially with emphasis on the oxide phase identification.

3. Experimental

Cast polycrystalline binary and ternary iron aluminides of composition Fe-15at.%Al to Fe-26at.%Al with alloying elements of Ta, Ti and Nb were used for oxidation experiments. All samples were produced by inductive melting and prepared as described by Pöter et al. [9]. As reference samples for adjusting the measurement set-up at the DELTA diffractometer beamline model oxides of 250-300 nm thickness consisting of Fe_2O_3 (hematite) on a Pt substrate were produced as described by Asteman et al. [10]. For all grazing incidence X-ray diffraction (XRD) measurements the incidence angle was 0.2° and synchrotron radiation of 13 keV was used.

3. Results

a. Measurements of thin oxide layers grown on binary and ternay iron aluminides at 700°C to 900°C

Fe-15at.%Al samples oxidised at 700°C, 800°C and 900°C for 5 hours yield a two layered oxide scale of Fe_2O_3 and Al_2O_3 composition. According to X-ray photoelectron spectroscopy (XPS) investigations, the thickness of the upper Fe_2O_3-rich layer is approximately 40 nm whereas the Al_2O_3 beneath is about 60 to 80 nm thick [9]. Figures 1 to 3 show the corresponding gracing incidence diffractograms indicating that hematite (Fe_2O_3) and corundum (Al_2O_3) are the main oxide phases present in the oxide layers grown at 700-900 °C after 5 hours reaction time. Surprisingly, no Al_2O_3 polymorphs like

γ- or θ- Al_2O_3 were detected. Most likely, this is due to the formation of fast growing hematite (Fe_2O_3) during the initial stage of oxidation acting as a precursor phase for the crystallisation of isostructural corundum (Al_2O_3).
In addition to phase identification, the XRD spectra yield information on the crystallinity of the grown oxide phases. α-Al_2O_3 and α-Fe_2O_3 formed at 700 and 800 °C are less crystalline than those grown at 900 °C as indicated by the larger peak width for both oxide phases (Fig. 1, 2, 3). This observation agrees with the oxide morphology found on the sample surface by FE-SEM. Corundum and hematite crystallized at 700 and 800 °C exhibit grains less than 100 nm in size, whereas at 900 °C larger, partly idiomorphous α-Al_2O_3 and α-Fe_2O_3 crystals are present on the sample surface.

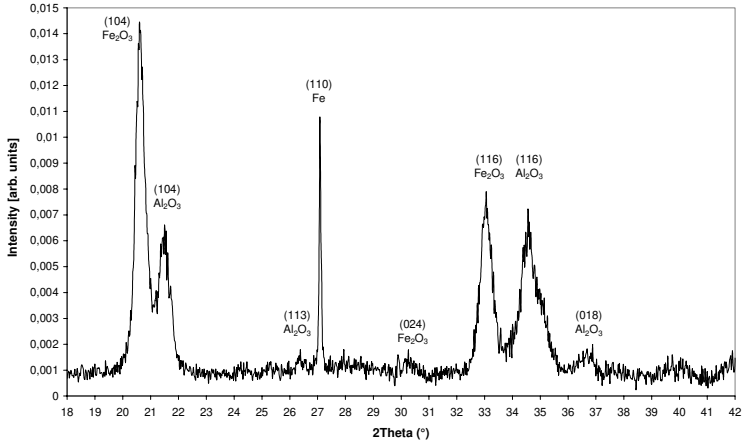

Fig.1 Fe-15at.%Al oxidised at 700°C / 5h / syn.air; incidence angle (θ) = 0,27° (interaction depth ~ 600 nm); phases identified: hematite (Fe_2O_3), corundum (Al_2O_3) and bulk material (α-Fe structure)

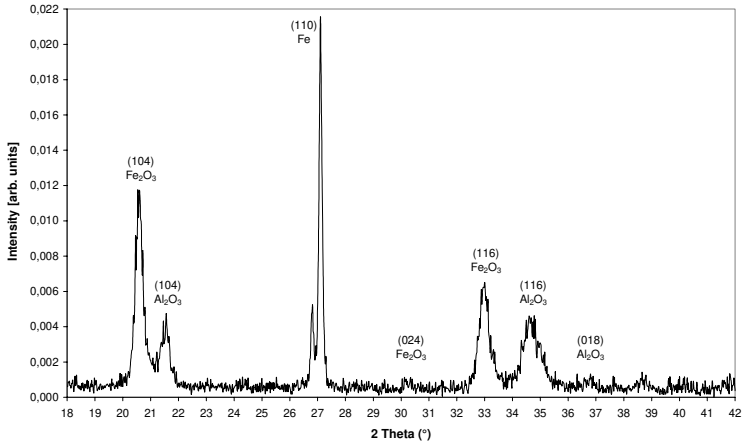

Fig.2 Fe-15at.%Al oxidised at 800°C / 5h / syn.air; incidence angle (θ) = 0,20° (interaction depth ~ 450 nm); phases identified: hematite (Fe_2O_3), corundum (Al_2O_3) and bulk material (α-Fe structure)

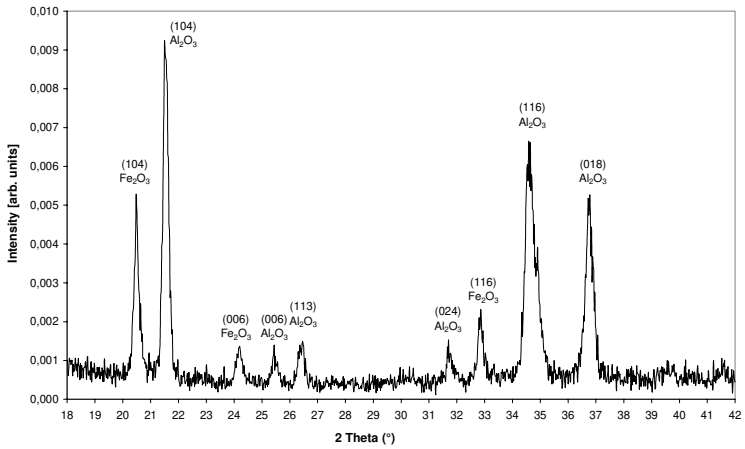

Fig.3 Fe-15at.%Al oxidised at 900°C / 5h / syn.air; incidence angle (θ) = 0,20° (interaction depth ~ 450 nm); phases identified: hematite (Fe_2O_3) and corundum (Al_2O_3)

In addition to Fe-15at.%Al, samples of the compositions listed in Table 1 were analysed.

Sample	**Oxidation**	**Oxide Phases identified**
Fe-25Al	700°C / 24h / $80N_2$-$20O_2$	hematite (Fe_2O_3) + corundum (Al_2O_3)
Fe-26Al-4Ta	700°C / 24h / $80N_2$-$20O_2$	hematite (Fe_2O_3)
Fe-26Al-4Ti	700°C / 24h / $80N_2$-$20O_2$	hematite (Fe_2O_3) + corundum (Al_2O_3)
Fe-26Al-4Nb	700°C / 24h / $80N_2$-$20O_2$	hematite (Fe_2O_3) + corundum (Al_2O_3)

Tab. 1 (Compositions given in at.%)

The oxide phases present on these intermetallics also consist of hematite (Fe_2O_3) and corundum (Al_2O_3) with the exception of Fe-26Al-4Ta where Fe_2O_3 is the main oxide phase occurring within the oxide layer (Fig. 4 to 6). Reflexes of the bulk material (Fe3Al intermetallic and Laves phase in the case of Ta and Nb addition) are only detected for the ternary iron aluminides indicating that the oxidation kinetics for these intermetallics is slower in comparison to the binary Fe-25Al alloy.

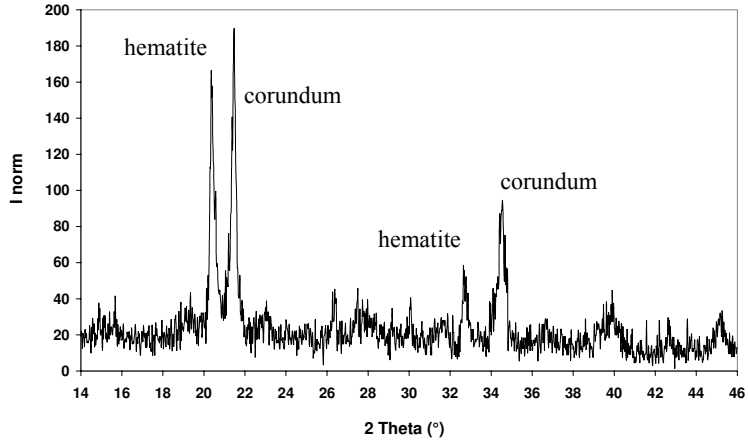

Fig.4 Fe-25Al oxidised at 700°C / 24h / syn.air; incidence angle (θ) = 0,20° (interaction depth ~ 450 nm); oxide phases identified: hematite (Fe_2O_3) and corundum (Al_2O_3)

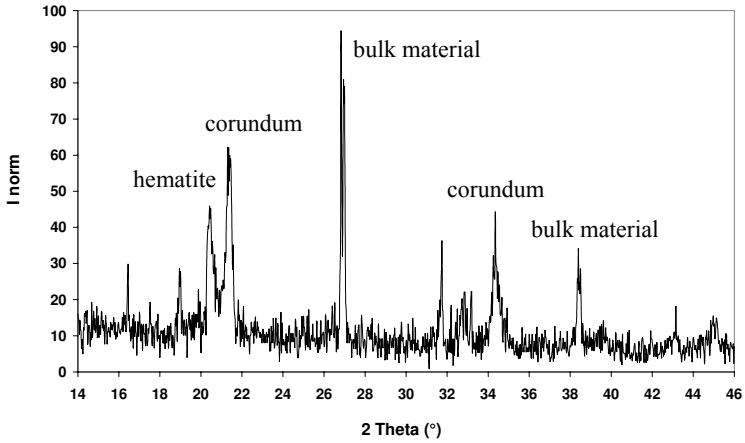

Fig.5 Fe-26Al-4Ti oxidised at 700°C / 24h / syn.air; incidence angle (θ) = 0,20° (interaction depth ~ 450 nm); oxide phases identified: hematite (Fe_2O_3) and corundum (Al_2O_3)

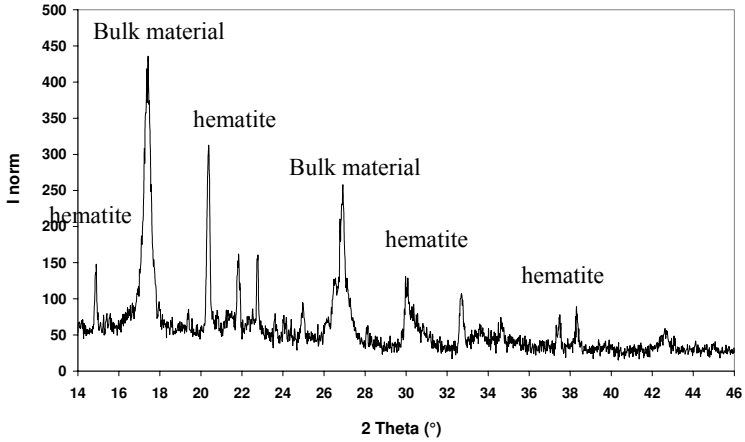

Fig.6 Fe-26Al-4Ta oxidised at 700°C / 24h / syn.air; incidence angle (θ) = 0,20° (interaction depth ~ 450 nm); oxide phases identified: hematite (Fe_2O_3)

b. Measurements of thick oxide layers grown on binary iron aluminides at 1000°C / 1000h

The oxide layer of an iron aluminide sample Fe-15at.%Al oxidised at 1000°C for 1000 hours was analysed with varying incidence angles in order to determine compositional variations with increasing oxide layer depth. Measurements were performed in the 2θ range of 20,2-21,8° ((104) reflexes of hematite and corundum) as well as 26,0-28,8° ((113) reflex of corundum). Results are shown in Fig. 7 and indicate that an increase of the incidence angle in the range 1-2° θ leads to a decrease in the hematite/corundum ratio. Thus the oxide layer seems to contain a larger amount of hematite than corundum in the upper part of the layer which corresponds to results obtained from short term oxidation experiments [9].

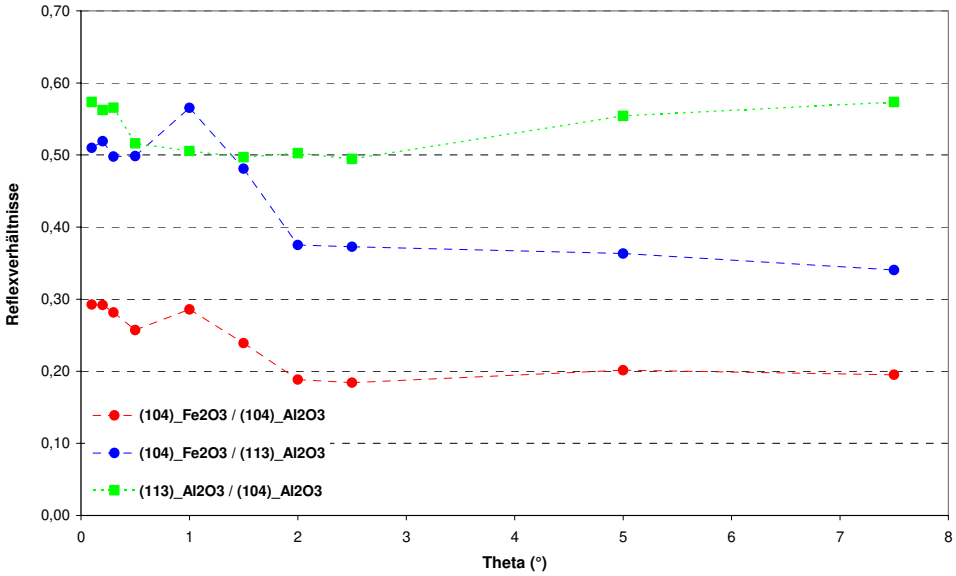

Fig.7 Hematite/Corundum ratio of reflex intensities with varying incidence angle of the XRD measurement for Fe-15at.%Al oxidised at 1000°C / 1000 h in syn. air

The corresponding interaction depth is given in Fig. 8 and varies between 300 nm up to 12 µm for the present measurements. In accordance with Fig. 7 it can be concluded that the hematite amount within the oxide layer decreases in the range between 2,5 and 5 µm depth.

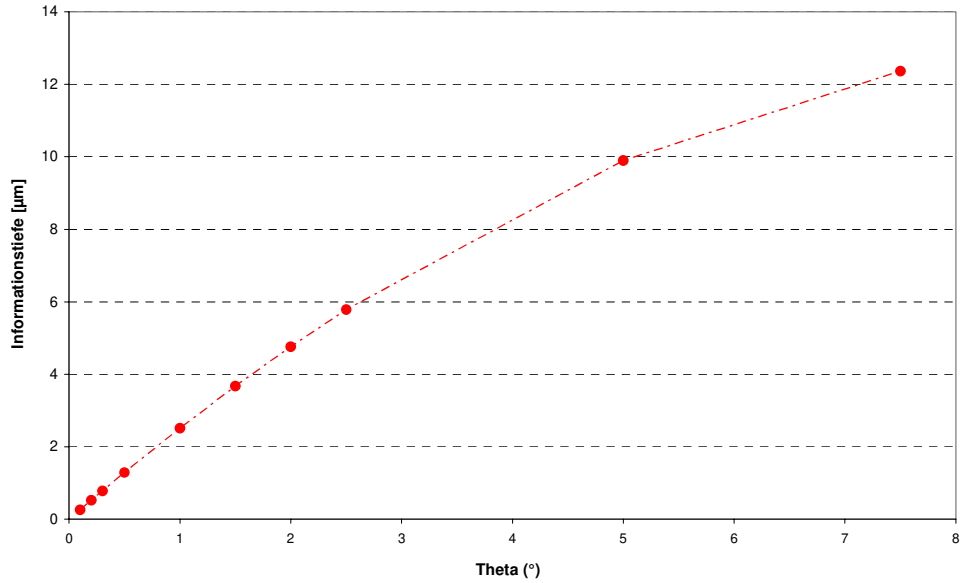

Fig.7 Interaction depth for gracing incidence XRD measurements depending on the incidence angle θ

Literature

[1] H.J. Grabke: *Intermetallics, **7** (1999)* 1153

[2] N. Babu, R. Balasubramaniam, A. Gosh: *Corr.. Sci.,* **43** (2001) 223

[3] M.A. Montealegre, J.L. González-Carrasco, M.A. Muñoz-Morris: *Intermetallics,* **9** (2001) 487

[4] F. Lang, Z. Yu, S. Gedevanishvili, S.C. Deevi, T. Narita: *Intermetallics,* **11** (2003) 697

[5] A. Velon, I. Olefjord: *Oxidation of Metals,* **56** (2001) 425

[6] W. Gao, Z. Li. Z. Wu, S. Li, Y. He: *Intermetallics,* **10** (2002) 263

[7] V. Shankar Rao, R.G. Baligidad, V.S. Raja: *Intermetallics , **10*** (2002) 73

[8] V. Shankar Rao, M. Norell, V.S. Raja: *Corr. Sci.*, **45** (2003) 2717

[9] B. Pöter, F. Stein, R. Wirth, M. Spiegel: *Z. Phys. Chem*. **219** (2005) 1

Structural properties of epitaxial Gd/Y alloy films grown on Al_2O_3

Arndt Remhof, Gregor Nowak, Alexei Nefedov, Kurt Westerholt and Hartmut Zabel

Institut für Experimentalphysik/Festkörperphysik,
Ruhr-Universität Bochum, D 44780 Bochum, Germany

Due to their partially filled 4f electron shells, the heavy rare earth (RE) metals possess complex magnetic phase diagrams. In Gd/Y alloys there is a competition between the ferromagnetic order favored by pure Gd films and the helimagnetism found in Y rich alloys. The existence and the characteristics of the magnetic phases are related to the crystal lattice, especially to the c/a ratio. Both Gd and Y crystallize in hexagonal closed packed (hcp) lattices with c/a=1.591 and c/a=1.571, respecticely. Therefore it is believed that in thin film systems a modification of the structure due to epitaxial stresses or clamping may effect the magnetic behavior.
In the following we present a detailed structural characterization of a 2000 Å thick $Gd_{40}Y_{60}$ alloy film grown on a Nb(110)/Al_2O_3(11-20) substrate by molecular beam epitaxy. The X-ray measurements were carried out at BL9 of the DELTA synchrotron radiation facility in Dortmund, Germany [1]. Key properties are the film thickness, the lattice parameters (in plane and out- of plane), the relative orientation of the crystal structures of film and substrate (i.e. the epitaxial relation), the coherence length and the interface roughness.

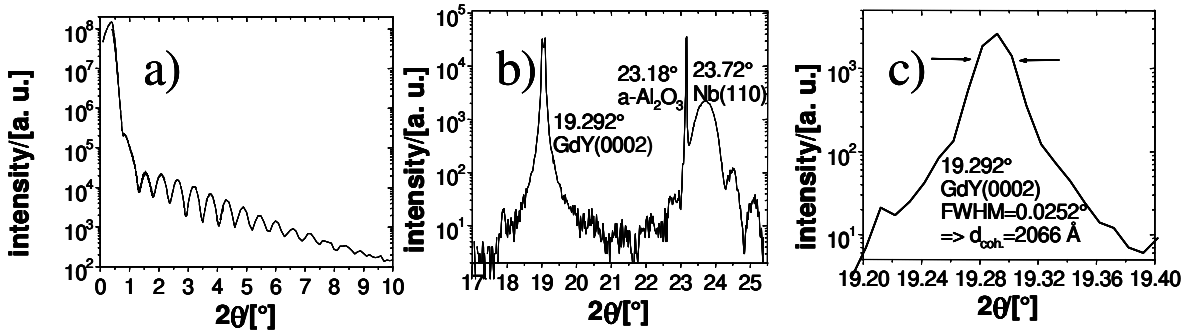

Figure 1: a) represents the reflectivity curve, b) shows a high angle radial scan (θ/2θ-scan). Panel c is a close-up of the GdY-reflection of panel b.

Figure 1a depicts the small angle reflectivity scan of the $Gd_{40}Y_{60}$-sample. This scan probes the electron density depth profile and yield the electron density, the thickness and the interface roughness of the consequent layers. Panel b shows a radial scan aligned with respect to the Gd/Y (0001) planes (c-axis). From small to high angles the GdY(0002), Al203(11-20) and the Nb(110) Bragg reflections can be identified. The presence of all three Bragg reflections confirm parallel growth of the respective lattice planes. The positions of the peaks corresponds to the lattice parameter and their width to the coherence length. The splitting of the $Gd_{40}Y_{60}$-peak is due to detector saturation. The Nb-reflection is accompanied by finite size oscillations, which would be more obvious using

a weaker absorber. Figure 1c is a close-up of panel 1b, showing the $Gd_{40}Y_{60}$(0002) reflection in more detail and with an appropriate absorber. From the FWHM a coherence length of about 2000 Å could be estimated, which corresponds to the nominal film thickness, indicating high crystalline quality

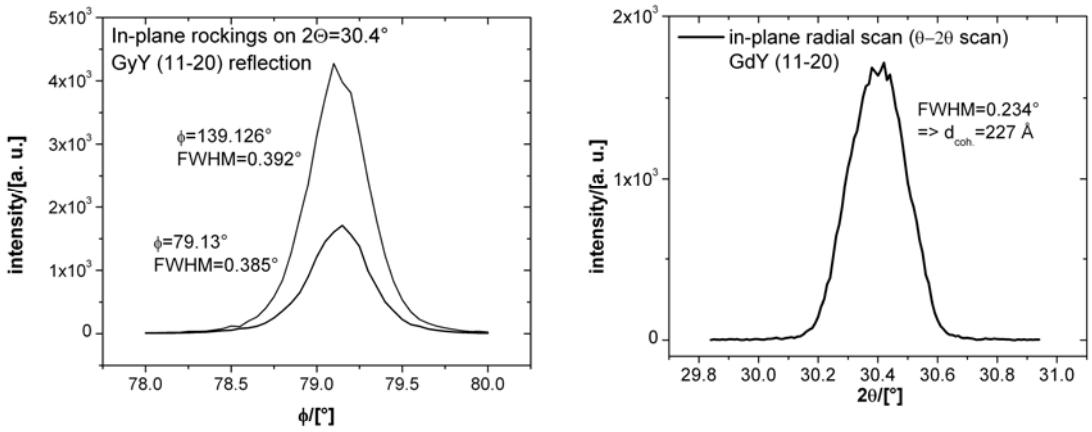

Figure 2: In-plane rocking (left) and θ–2θ-scans (right)

To measure the epitaxial relations, the in-plane coherence length and the in-plane mosaicity, gracing incident x-ray diffraction (GIXRD) has to be carried out. Usually the in plane structure of thin metallic films is less well defined than the out-of plane structure, leading to broader diffraction peaks. Figure 2 (left panel) shows two superimposed $Gd_{40}Y_{60}$ Bragg reflections, separated by 60° in ϕ, indicating the six-fold symmetry of the $Gd_{40}Y_{60}$ crystal. The different intensities have geometrical origin. The in plane coherence length can be calculated from in-plane radial scans (see fig.2, right panel). The estimated value of 227 Å is a good value for a metallic thin film and typical for the rare earth metallic films grown on single crystalline Nb buffers. From the angular position of the respective in-plane and out-of plane the c/a can be calculated to 1.565, which is about 1% smaller than the value of the bulk alloy.
To summarize, we demonstrated the possibility to prepare single crystalline, epitaxial Gd/Y alloy films on Nb/Al_2O_3 substrates. Magnetically they exhibit ferromagnetic order at Y concentrations below 48%. At higher Y-concentrations the alloy orders in an antiferromagnetic helix. The magnetic ordering temperature decreases with increasing Y concentration. We attribute deviations to the bulk magnetic phase diagram to the modified lattice parameters induced by the substrate.

We gratefully acknowledge the distinct support by Martin Volmer, Michael Paulus and Christian Sternemann during the experiment.

[1] C. Krywka, M. Paulus, C. Sternemann, M. Volmer, A. Remhof, G. Nowak, A. Nefedov, B. Pöter, M. Spiegel, and M. Tolan, 'The new diffractometerfor surface x-ray diffraction at beamline BL9 of DELTA', J. Synchrotron. Rad., accepted.

Influence of interface structure on spin-density-wave magnetism in Cr/Ni bilayers

A. Nefedov, E. Kravtsov, A. Remhof and H. Zabel

Institut für Experimentalphysik/Festkörperphysik, Ruhr-Universität Bochum, 44780 Bochum, Germany

During the last years the spin-density-wave (SDW) magnetism in thin Cr films and in multilayers has attracted much interest resulting in intensive investigations. It should be noted that whereas the SDW behaviour in bulk Cr is well established by now (see review [1] and references therein), there are significant gaps in our understanding of magnetism in thin Cr layers contacting with layers of other metals [2]. The most significant factors affecting the SDW state in Cr thin film systems are non-ideal interface structures and proximity effects from neighbouring layers. Cr/Ni bilayer is a system, in which the SDW state is expected to be under strong influence of proximity effects at the Cr-Ni interface. The present research is aimed to investigate systematically proximity and interface effects in Cr/Ni systems and to trace a correlation between interface structure and SDW state in Cr/Ni bilayers.

As the first step in this program, we have investigated the influence of growth conditions on structural properties of Cr/Ni bilayers. To our best knowledge, the problem of growth of fcc Ni films on bcc Cr(001) has not yet been addressed in experimental investigations and there was no information about proper growth conditions and possible epitaxial relationships. Our results are the first ones in this direction.

The measurements were done on a series of Cr(2000 Å)/Ni(40 Å) bilayers grown with MBE methods at different temperatures on MgO(001) substrates, which are expected to have different Cr-Ni interface structures. The growth temperature range (from 50^{o}C to 500^{o}C) was chosen in such a way to cover a large variety of possible interface types from geometrically rough to diffusively intermixed ones. The most optimal growth with sharp interfaces and unique epitaxial relation may thereby be found. The Ni/Cr epitaxial relationship and interface structure in the bilayers were determined with x-ray diffraction studies done at SAW (DELTA) and W1.1 (HASYLAB) beamlines.

As evident from the scans presented in Figure 1, the Cr/Ni growth was found to induce a tetragonal Ni lattice distortion corresponding to 3% lattice expansion in the out-of-plane direction and 2% in-plane compression as compared with bulk Ni. The epitaxial relationship for the Cr(001)/Ni system is as follows: Cr(100)//Ni(110) and Cr(001)//Ni(1-10) in-plane and out-of-plane, respectively. The X-ray measurements have revealed a direct correlation between the Ni crystal structural quality and growth temperature conditions. The optimal growth temperature providing the best Cr/Ni interface structure was established to be about 120^{o}C. Decrease in the

growth temperature below the optimal value causes significant increase in interface roughness, whereas increase in the growth temperature leads to strong Cr-Ni intermixing near the interface.

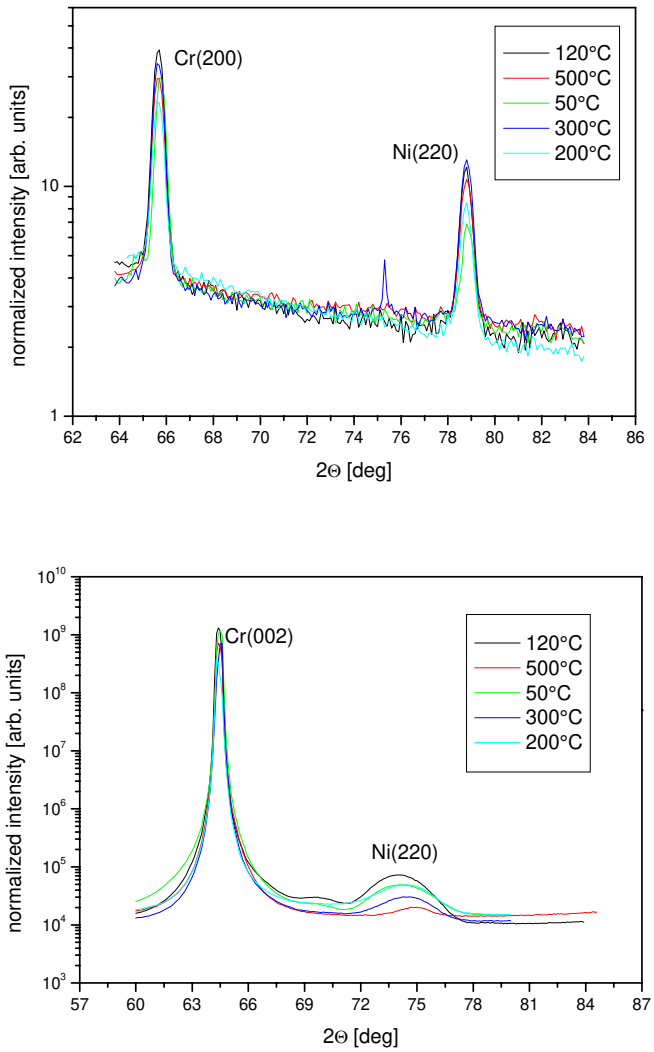

Fig. 1. X-ray scans through the in-plane (a) and out-of-plane (b) Cr/Ni Bragg peaks (λ=1.542Å).

Neutron scattering experiments done at UNIDAS instrument (FZ Jülich) provide us clear experimental evidence for a strong influence of the Cr/Ni interface structure on the spin-density-wave magnetism in rather thick Cr films. We have detected that thin Ni films grown at optimal temperature of 120°C on top of a 2000 Å- thick Cr film does not change the SDW behavior as compared with similar plain Cr films without Ni cover. However, non-perfect Cr/Ni interface structures affect both the SDW polarization (intermixed interface) and propagation direction (rough interface).

References

[1] E. Fawsett, Rev. Mod. Phys. **60**, 209 (1988).
[2] H. Zabel, J. Phys: Condens. Matter **11**, 9303 (1999).

Experimental report: Measurements at beamline BL09 @ DELTA 26.-28.09.2005 – Structure peaks of poly(propylene glycol)

S. Streit*, M. Paulus, and M.Tolan
Exp. Physik Ia, Universität Dortmund, Otto-Hahn-Str. 4, 44221 Dortmund, Germany
* Corresponding author: streit@physik.uni-dortmund.de

The bulk structure factor of the glass forming polymeric liquid poly(propylene glycol) (PPG) with a molecular weight of 400 kg/mol was investigated by grazing incidence diffraction (GID) in a liquid scattering setup at the beamline BL09 at DELTA at an energy of 10.05 keV in a temperature range reaching from room temperature to below the glass transition temperature of PPG, $T_G \sim 180$ K. The aim of the experiment was to investigate the temperature dependence of lateral correlations of the surface structure on atomic length scales, induced by thermally activated capillary waves, around the glass transition. Three weeks earlier, surface GID measurements of PPG-400 have been performed at the ESRF, but in order to calculate the surface tension, it is necessary to determine the influence of the structure peak, thus additional measurements at DELTA were of essential importance.

In earlier studies the statics of liquid surfaces have been investigated extensively by measuring the time-averaged roughness with x-ray reflectivity measurements [1]. With the increase of synchrotron flux as well as the improvement in the instrumentation, the detection of off-specular diffuse scattering has become possible as well. While at micrometer scales fluctuating matter behaves according to the continuum classical hydrodynamic theory, at nanometer scales strong deviations from this theory are predicted [2]. At very small length scales the capillary wave model is no longer valid, so the small-scale surface structure is modelled by a wavevector dependent surface energy which has already been observed for different molecular liquids [3], but for highly viscous liquids and glasses a systematic study is still missing.

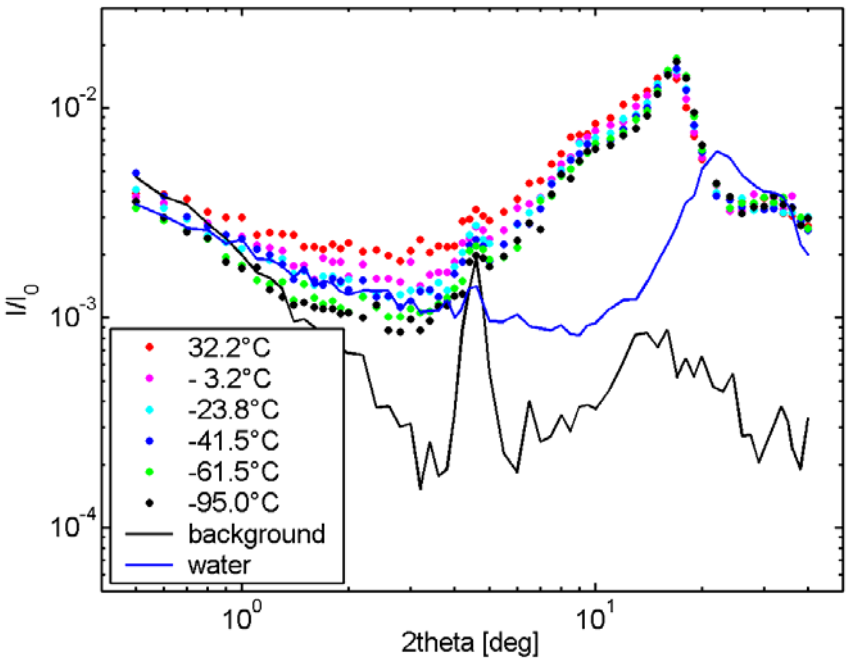

Fig. 1: All measured diffuse raw data of PPG-400 and water, together with the not yet substracted background measurements.

The sample was injected with a micropipette into a U-shaped copper sample holder, equipped with Kapton windows at the front and the back to allow x-ray transmission. The sample was about 2 mm thick, leading to a transmission of about 50% at 10 keV. The sample holder which was kept under vacuum was screwed onto a cryostate for temperature open-loop control, resulting in a sufficient accuracy of ± 0.4 K. A beamstop just after the exit windows of the sample cut off the direct beam, thus diminishing air

scattering outside the sample cell. Measurements of about 2 hours in an in-plane-of-incidence geometry ranging from 2θ = 0.5° to 40° - corresponding to a wavevector transfer parallel to the sample surface $q_{||} \sim 0.04$ to 3.0 $Å^{-1}$ - were performed at T = 305 K, 295 K, 270 K, 249 K, 232 K, 212 K, and 178 K, respectively. Additionally a reference measurement with water and three background scans with an empty sample holder were accomplished.

The preliminary results of the measurements are shown in figure 1. It was found that the position of the structure peak is mostly independent of temperature, but for small wavevector transfers q a systematical decrease of intensity with decreasing temperature was observed. Also a slight broadening of the structure factor with increasing temperature occurred, which can be explained by the fact that the mean distance of the polymer subgroups is not well defined due to the increased mobility at higher temperatures. For application of the structure factor subtraction in the ESRF data, all scans at different temperatures were summed up as shown in figure 2. A further analysis of the data is still in progress.

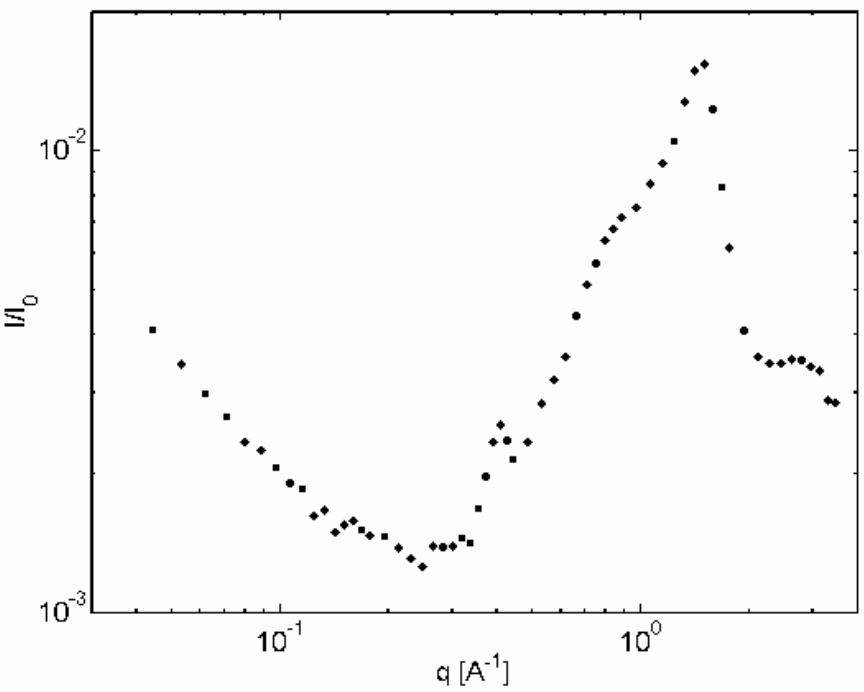

Fig. 2:
PPG raw data, summed up for all temperatures in order to increase the statistics.

The presented results, in combination with recently performed GID measurements of the surface of PPG-400 at the ESRF, should help to complete a theoretical description of the glass transition of PPG by calculating its temperature-dependent surface tension, thus leading to a complete description of the liquid surface structure on atomic length scales.

References

[1] M. Sprung, T. Seydel, C. Gutt, R. Weber, E. DiMasi, A. Madsen, M. Tolan: *Surface roughness of supercooled polymer melts*, Phys. Rev. E **70**, 051809 (2004).

[2] M. Napiórkowski, S. Dietrich, Phys. Rev. E **47**, 1836 (1993); K. Mecke, S. Dietrich: *Effective Hamiltonian for liquid-vapor interfaces*, Phys. Rev. E **59**, 6766 (1999).

[3] S. Mora, J. Daillant, K. Mecke, D. Luzet, A. Braslau, M. Alba, B. Struth: *X-ray synchrotron study of liquid-vapor interfaces at short length scales: Effect of long-range forces and bending energies*, Phys. Rev. Lett. **90**, 216101 (2003).

Ultra-thin Isobutane films on Si substrates

Kaveh Shokuie, Robert Fendt, Michael Paulus, Christian Sternemann, Metin Tolan

Lehrstuhl für Experimentelle Physik 1, Universität Dortmund

Experimental report:

We report on recent X-ray reflectivity experiments, performed at beamline BL9 (SAW2) of DELTA in June 2005. thin Isobutane films on silicon substrates were prepared using a newly designed sample cell. X-ray reflectivity is a powerful technique that allows to determine a sample's electron density profile perpendicular to the sample's surface with highest precision [1-3].

Isobutane is gaseous under normal conditions. However, near the substrate one observes a thin layer of adsorbed Isobutane in a condensed state. The properties of this layer such as e. g. thickness and roughness strongly depend on the thermodynamic state of the gas. This means that the film can be changed by controlling either the temperature of the system or the pressure. In the case of Isobutane films of different thickness can be prepared by means of increasing the pressure to about 2-3 bar.

In X-ray reflectivity, the wavevector transfer $\vec{q}$ only consists of a component perpendicular to the sample surface. Therefore, the technique yields the electron density profile perpendicular to the sample's surface while averaging laterally (the lateral structure of the sample is obtained only indirectly by fitting e. g. the film's roughness). However, a film's thickness can be determined with Ångstrom precision. X-ray scattering techniques in general are non-destructive probes allowing in-situ measurements on soft-matter systems. Thus, X-ray reflectivity is the ideal tool for our purpose.

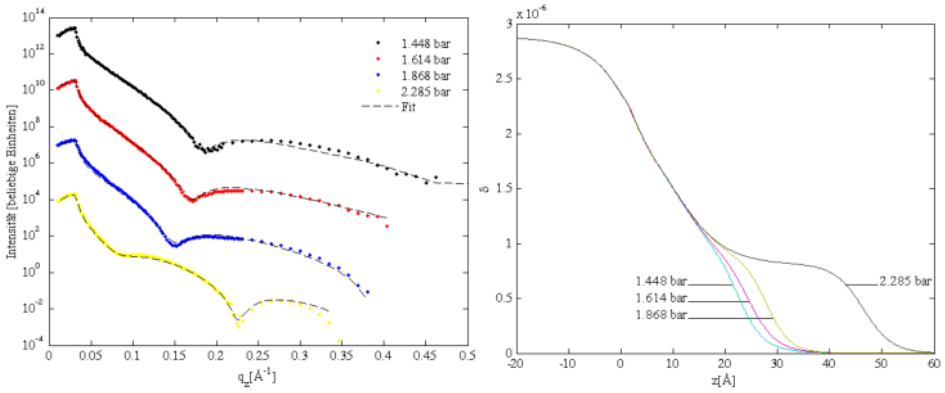

Figure 1a: Reflectivities of Isobutane films adsorbed on Silicon at different pressures.
Figure 1b: Density profiles of the system at different pressures calculated from the data of the fit.

Since in the case of Isobutane the key parameter for controlling the film thickness is the pressure, it is possible to measure different films at constant temperature. The correlation between pressure and film thickness has been measured, yielding as a result the sample's adsorption isotherm. The experimental results were compared to calculations according to the Frenkel-Halsey-Hill (FHH) model [4-7].

Figure 1a shows the 4 reflectivities that were taken from Isobutane on a silicon wafer with native oxide layer at the beamline BL9 at DELTA. The dashed lines represent the fits. From this fits the density profiles (fig. 1b) and the resulting isotherm were determined (fig. 2). Figure 2 also shows

fits of the calculated isotherm according to the FHH model.

According to FHH theory, the layer thickness d can be calculated as

$$d = \left(\frac{\alpha}{k_B T \ln \frac{p_0}{p}} \right)^{\frac{1}{3}},$$

depending on the pressure p, the codensation pressure p_0, the temperature T, and the strength of the interaction between substrate and adsorbate, α. k_B denotes Boltzmann's constant.

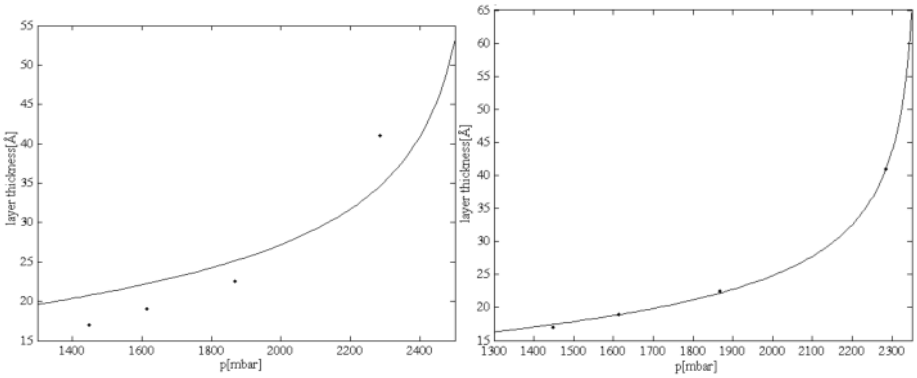

Figure 2: Absorption isotherms of Isobutane on a Si substrate. The solid lines represent fits according to the FHH-Model. The left fit only consideres α, the right fit both α and p_0 as fit parameters.

In the left fit only α was used as fit parameter with fixed T=298,15 K while in the right fit α and p_0 were fitted. The choice for p_0 as fit parameter is plausible since a temprature gradient during the measurement was observed, which essentially means that the substrate has had a different temperature than measured. If one assumes that the substrate temperature was different (e. g. lower), one gets a different condensation pressure as a result. If this is taken into account, the agreement between model and measured data is very good, yielding a sample temperature which is about 1-2 K lower than the measured value.

In summary, we showed that the measured data can be understood within the scope of the FHH theory. However, recent experiments utilising X-ray photon correlation spectroscopy (XCPS) suggest that the behaviour of adsorbed alkane films is not as simple as assumed [8]. In view of these results, highest-resolution static measurements of these systems become increasingly important. Our experiment has shown that the DELTA source is well-suited for such measurements.

References:

[1] PARRATT, L. G.: Physical Review 95 , 359 (1954)
[2] HOLY, V.; PIETSCH, U.; BAUMBACH, T.: High-Resolution X-Ray Scattering; 2nd edition. Springer (2004)
[3] ALS-NIELSEN, J; MCMORROW, D.: Elements of Modern X-Ray Physics. Wiley-VCH (2001)
[4] FRENKEL, J.: Kinetic Theory of Liquids. Clarendon (1946)
[5] HALSEY, G. D.: J. Chem. Physics 16, 931 (1948)
[6] HILL, T. L.: J. Chem. Physics 17, 590 (1949)
[7] MECKE, K. R.; KRIM, J.: Phys. Rev. B 53, 2073 (1996)
[8] FENDT, R; GUTT, C.: XPCS measurements at ESRF and APS; unpublished

The x-ray small angle scattering setup at BL9 of DELTA: First measurements of Lysozyme solutions

C. Krywka[1,*], C. Sternemann[1], N. Javid[2], R. Winter[2], M. Tolan[1]

[1] Institute of Physics / DELTA, University of Dortmund, D-44221 Dortmund, Germany
[2] Institute of Chemistry, University of Dortmund, D-44221 Dortmund, Germany
[*] corresponding author: christof.krywka@uni-dortmund.de

(October 2005)

The biological activity, thermodynamic stability and the physical and chemical properties of proteins are strongly influenced by the structure of dynamics of their aqueous microenvironment [1]. Hence, understanding the effects of various types of cosolvents typical for cellular conditions on the structure and dynamics of proteins is crucial for a deeper insight into protein folding as well as aggregation processes, which play an important role in many conformational diseases, such as Alzheimer, Huntington, Creutzfeldt-Jakob, and Parkinson. Recently, it was shown that the latter processes are in fact strongly influenced by the type and concentration of cosolvents [2]. The purpose of this experiment is to obtain detailed information about the structure of the hydration shell of Lysozyme in aqueous solution in a wide concentration range in the presence of different types of cosolvents and, for the higher concentrated samples, information about the intermolecular interaction potential from the measured structure factors.

A new setup for small angle x-ray scattering (SAXS) has been built up and commissioned during October 2005 at the beamline BL9 (SAW2) of DELTA, utilizing a MAR 345 image plate detector. The monochromatized x-ray beam of 13 keV energy was focused at the detector position and collimated to a size of 0.8×1 mm^2 (vertically $\times$ horizontally) using two slit systems. An automatic shutter and absorber set (XIA PF2S2+PF4) is placed in between these slit systems. Samples can be filled either into quartz capillaries or into cavities encircled by a gold coated copper frame enclosed by two MICA windows. The samples can be temperature controlled in a range of -10 °C to 80 °C. Air scattering at the beampath was reduced by extensible tubes filled with helium. The measured intensity can be normalised to the signal of a NaI monitor detecting the air scattering of the direct beam. The lead beamstop is held in place by a Kapton foil spread across the active area of the MAR detector and is directly positioned in front of the MAR detector. The sample to detector distance can be varied over a wide range of 0.3 to 3.2 m. Detector tilt, detector to sample distance and direct beam position were

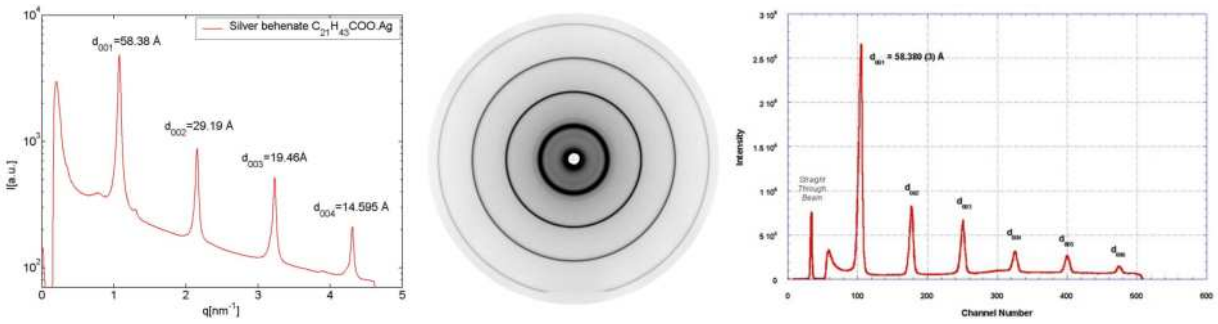

Figure 1: Left: integrated scattering intensity of the silver behenate calibrant, exposure time was 60s. Middle: raw 2D scattering data. Right: ESRF reference data [3].

calibrated by measuring the powder diffraction pattern of silver behenate ($C_{21}H_{43}COO.Ag$, purchased from Rose Chemicals LTD, UK). The powder was filled into a quartz capillary and placed in the sample holder. The diffraction pattern was measured at different detector to sample distances, in Fig. 1 the distance is 2450 mm, hence the maximum measured momentum transfer q is about $0.46\mathring{A}^{-1}$. The peak positions are in very good accordance to the known d_{00l} spacings [3]. The calibration was performed from the diffraction data utilizing the program package FIT2D [4].

First measurements of aqueous Lysozyme solutions at a wide concentration range between 1 wt. % and 20 wt. % were accomplished at a detector to sample distance of 3.2 m, thus SAXS spectra could be measured for momentum transfers q between $0.01\mathring{A}^{-1}$ and $0.35\mathring{A}^{-1}$, the lower limit being defined by the size of the beamstop. The scattered intensity of the pure solvent (20 mM citrate buffer, pH 4.6) was subtracted from the scattering signal of the Lysozyme solution to account for background radiation. The difference signal was integrated using the program package FIT2D. Integrated spectra of Lysozyme solutions at different concentrations are shown in Fig. 2. The peak positions are in agreement with measurements previously performed at beamline X33 of EMBL (Hasylab, Hamburg) [5]. Further analysis of the data is in progress.

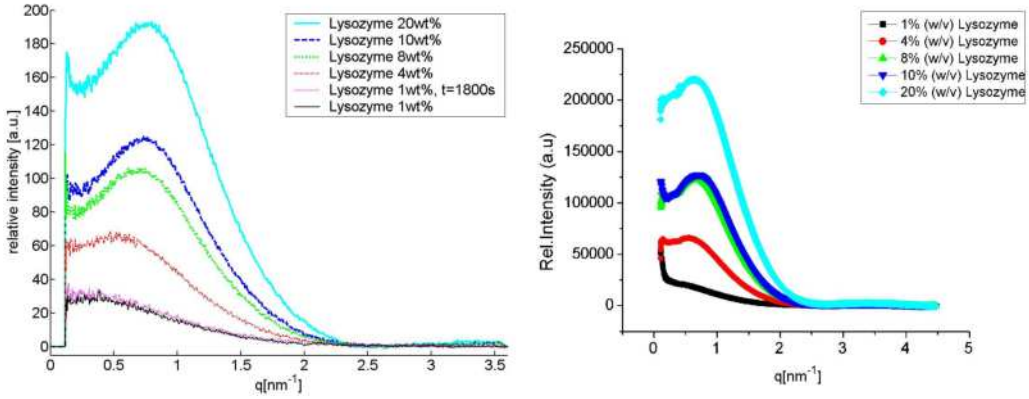

Figure 2: Left: SAXS spectra of aqueous Lysozyme solutions in 20mM citrate buffer at pH 4.6, T = 26.5° C, exposure time was 900 s, except the 1 wt. % solution which has also been irradiated for 1800 s. Right: Reference data taken at beamline X33 of EMBL (Hasylab) [5].

We have successfully performed SAXS measurements on aqueous solutions of Lysozyme with a mininum momentum transfer of about $0.01\mathring{A}^{-1}$. In this first approach background scattering was reduced by means of extensible He filled tubes, covering most of the beampath of the scattering radiation. Further optimization is required in order to improve the background to signal ratio, especially the direct beam air scattering at low q values. A better resolution in the low q regime and at the same time reduced exposure times are expected. With the improved setup we will perform measurements of Lysozyme solutions with added cosolvents in order to examine the changes of the structure of the protein and its hydration shell during the process of unfolding from the native state.

[1] R. B. Gregory (Ed.), Protein-Solvent Interactions, Marcel Dekker, New York, (1995).
[2] W. Dzwolak, R. Ravindra, R. Winter, PCCP **6**, 1938 (2004).
[3] T. C. Huang, H. Toraya, T. N. Blanton, Y. Wu, J. Appl. Cryst. **26**, 180 (1993)
[4] A. P. Hammersley, Syn. Rad. News **24**, (1989).
[5] N. Javid, private communication.

Synchrotron Radiation Induced X-ray Standing Waves

Markus Krämer [1)], Alex von Bohlen [1)], Christian Sternemann [2)] and Roland Hergenröder [1)]
1) ISAS – Institute for Analytical Sciences Dortmund, Bunsen-Kirchhoff-Str. 11, 44139 Dortmund
2) Experimentelle Physik E1a / DELTA, University of Dortmund,
Maria-Goeppert-Mayer-Str. 2, 44221 Dortmund, Germany

Abstract

The method of X-ray standing waves (XSW) is a technique for the characterization of thin films, layered structures and surface depositions on a nanometer scale. The essential requirements are a flat, well reflecting substrate and monochromatic coherent primary X-ray radiation (e.g. from a synchrotron). To perform an XSW measurement the sample to be observed is irradiated under grazing incidence while the angle is scanned continuously and the fluorescence radiation is observed. XSW measurements are fast and element specific. However, several elements can be observed simultaneously by an energy dispersive detector. For each angle the fluorescence radiation of the detected elements is recorded and the signals are plotted vs. the angle of incidence of the scan. The obtained curves represent a characterization in depth of the layer-structure of samples. XSW can be performed on conducting and non-conducting samples, and vacuum is not necessary in most cases. Thus samples can be characterized with little preparation.

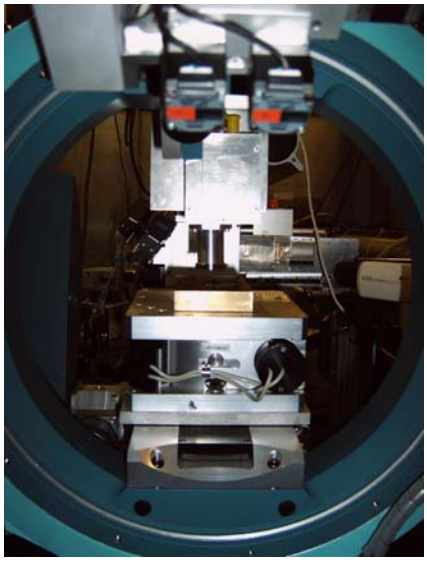

Fig. 1: Experimental set-up at DELTA.

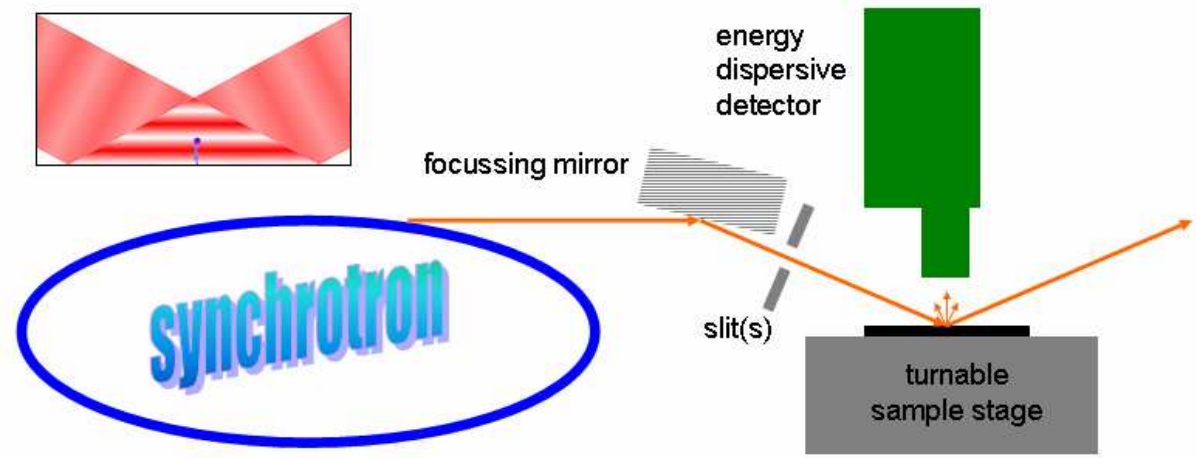

Fig. 2: Measurement principle and schematic illustration of the XSW field above the substrate (inset).

To extract information about the observed sample system from the measured scan it is necessary to calculate the theoretically expected fluorescence signal for a given sample system and fitting its parameters so that theoretical and experimental curve agree. For calculation of these theoretical curves a computer simulation has been developed (and is still being refined) that considers the physical properties of all the components in the sample system as well as diffraction and absorption of the radiation for all positions inside the sample and all angles of incidence of the exciting synchrotron radiation.

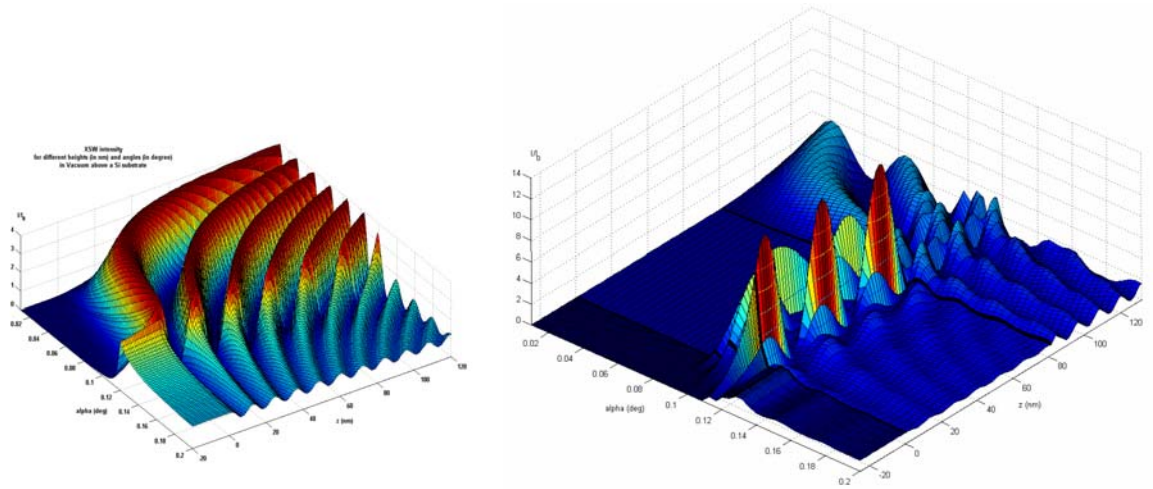

Fig. 3: Simulation of X-ray standing waves above a simple Si substrate (left) and in a layered sample of 1 nm Au on 80 nm polystyrene on 1 nm SiO_2 on a Si substrate (right).

During two beamtimes at DELTA various sample systems have been observed with this method, and measurements on known systems have shown that the computer simulation leads to realistic and accurate results.

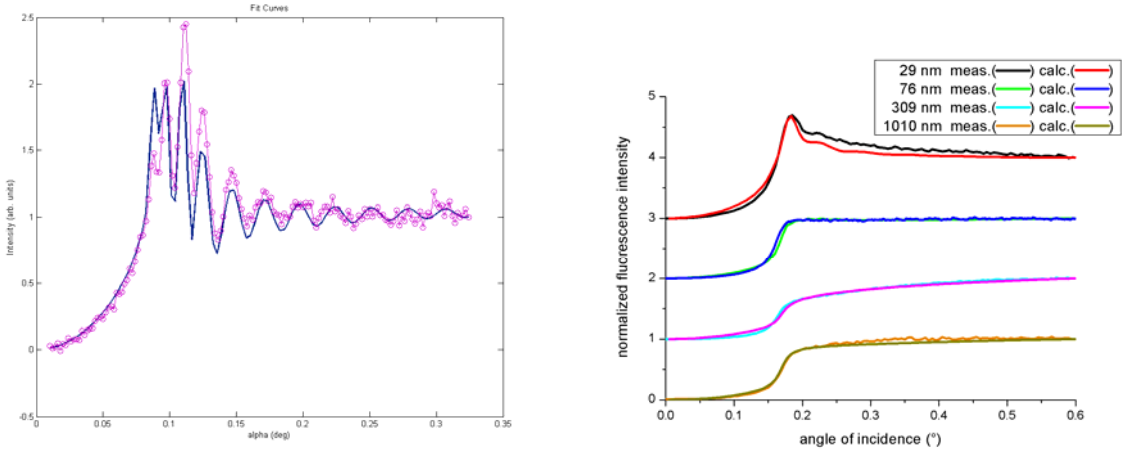

Fig. 4: Measurements and simulated curves for a layered sample of 1 nm Au on 80 nm polystyrene on 1 nm SiO_2 on a Si substrate (left) and for Si substrates covered with Ge layers of various thicknesses.

To simplify fitting procedures with several unknown parameters (as layer thicknesses or electron densities) evolutionary algorithms are intended to be included in the simulation program. Furthermore, a sample cell has been designed at ISAS that allows measurements under vacuum conditions or at a defined vapour pressure. The first method will increase the detected fluorescence intensity especially from light elements by preventing absorption in air between sample and detector. With the second method the thickness of a liquid layer on the sample can be varied or stabilized during XSW measurements by controlling the vapour pressure inside the cell.

Overall, XSW is an interesting and promising method for characterization of layered samples, both as a reference measurement to other X-ray techniques and as a possible alternative measurement for cases where other methods are not suitable or possible.

Synchrotron radiation induced X-ray micro fluorescence.

A. von Bohlen[1], M. Krämer[1], P. Jacob[1], R. Hergenröder[1], C. Sternemann[2], M. Paulus[2], M. Volmer[2], C. Krywka[2].

[1] Institute for Analytical Sciences – ISAS Dortmund, 44139 Dortmund, Germany
[2] Department of Physics / DELTA, University of Dortmund, 44221 Dortmund, Germany

The increased interest in spatial resolved X-ray fluorescence analysis in medicine, biology and material sciences demands special solutions. Sub-micrometer resolution combined with high sensitivity and monochromatic excitation at a wide range of energies can only be realized in a reasonable measuring time when applying synchrotron radiation (SR) as excitation source. The radiation supplied by beamline SAW 2 at DELTA was chosen for preliminary experiments carried out as feasibility study for diverse applications.

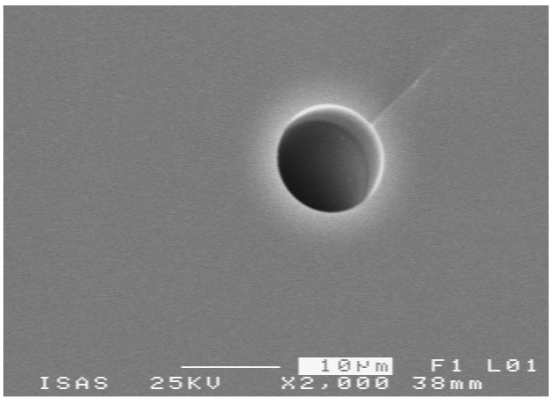

In a first step the implementation of simple mono-capillary optics for collimation and concentration of the SR via total reflection was tested at SAW 2 beamline. It could be shown that cylindrical capillaries made of borosilicate glass with at least 10 µm inner diameter can be used after alignment to produce excellent SR micro probes. Energies of 5, 13, 15, 22, and 30 keV were adjusted at SAW 2 beamline and were used after collimation by the capillary for excitation of the samples to X-ray fluorescence.

Fig. 1. SEM micrograph of a 10 µm mono-capillary

An application field was the non-contact and destruction free analysis of objects of cultural heritage. The material composition of two outstanding archaeological finds from the city area of Dortmund was characterized by using SR-EDXRF. The first object (cf. Fig 2), a decoration plate of a buckler used by the Germans living in the 4th century AC in this area was made of a silver plate decorated with silver pearls and gold foils. The pearls and foils were fixed with a tin solder onto the silver base. The provenance of the materials was deduced to be Scandinavia by regarding the historical background. A second object shown in Fig. 3, a recent find, is a brooch discovered in a cemetery attributed to Franken living in the area about 1500 years ago. The basic metal was pure silver. However, as could be shown by the micro-analytical characterization of some yellowish areas, the artefact was gilded. The inserted red-violet stones are Almandines ($Fe_3Al_2(SiO_4)_3$), a special type of garnet. The material of the central four white inserts could not be deduced unambiguously from the results of the elemental composition. A further characterization of the light elements – X-ray fluorescence radiation of C, O, N, F, Mg, Al, etc. is absorbed in the air of the set-up – has to be made. Otherwise it is impossible to decide if the material is glass or seashell.

Fig. 2. Ornament of a German buckler mounted in measuring position at SAW 2 beamline.

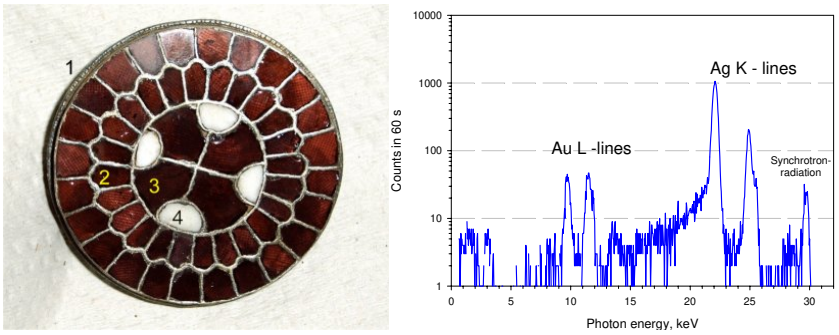

Fig 3. Brooch found in Dortmund-Asseln. Analyses were made on marked areas. Spectrum of a gilded metal part (2) showing silver and gold signals.

A further experiment concerns the detection of element solutions in micro-channels covered by polymer foils. The final goal of these experiments is to visualize the local distribution of diluted solution in capillaries and micro channels used for the 'lab on the chip'. It could be demonstrated that in this second application of SR induced X-ray fluorescence a 1% aqueous Molybdenum solution can be excited to X-ray fluorescence and the radiation can be detected through a PMMA foil of 300 µm thickness. A model of the set-up is shown in Fig. 4 and the real sample of a micro channel in Fig. 5.

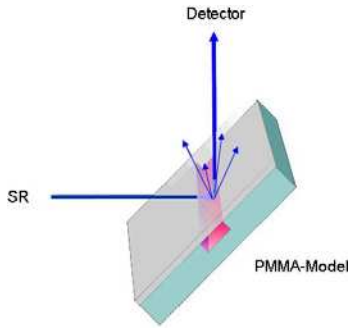

Fig. 4. Scheme of SR-XRF in buried channels

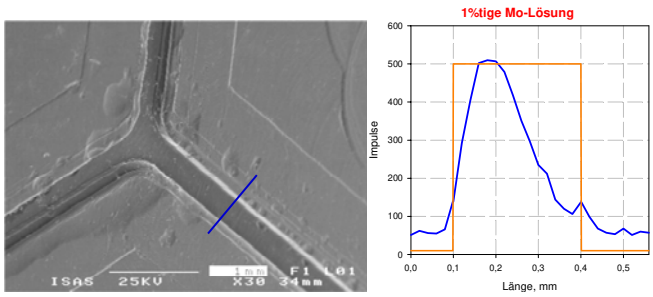

Fig. 5. A SEM micrograph of a micro channel on a PMMA substrate is shown. The elemental distribution over the blue line is represented in the right graph.

The last experiment carried out at BL 9 concerns the analysis of material without sample support. This was achieved by using an acoustical trap. Small amounts of liquids or tiny pieces of solids can be levitated in such a trap. The advantages of acoustical levitation as a general tool for sample manipulation (influence of temperature, pressure, reaction in different atmospheres, etc.) and possible applications of the technique for X-ray fluorescence, X-ray diffraction or absorption will be tested in the future.

Outlook

The results of these preliminary SR-EDXRF measurements encouraged us to build up a wavelength dispersive spectrometer attached to a vacuum chamber for SR induced micro-analysis of the light elements. The system will include X-ray optics of different types (mono-capillaries, poly-capillary lenses and refractive optics) for best spatial resolution and optimal excitation of the samples.

Structural and electronic analysis of Hf on Si(111) surface studied by XPS and XPD

M.F. Carazzolle[1,2], M. Schürmann[1], U. Berges[4], C. Flüchter[1], D. Weier[1], U. Berges[1], A. De Siervo[3], R. Landers[2,3], G.G. Kleiman[2], and C. Westphal[1,4]

[1]Experimentelle Physik 1 – Universität Dortmund, Otto-Hahn-Str. 4, D44221-Dortmund, Germany
[2]Instituto de Fisica - Universidade Estadual de Campinas, C.P.6165, 1083-970-Campinas, SP, Brazil
[3]Laboratorio Nacional de Luz Sincrotron, C.P. 6192, 13084-971-Campinas, SP, Brazil
[4]DELTA, Maria-Groeppert-Mayer-Str. 2, D44227-Dortmund, Germany

INTRODUCTION

The development of alternative high-k gate dielectrics for future complimentary metal-oxide-semiconductor (CMOS) devices is indispensable in achieving both low leakage current and small equivalent oxide thickness. The thermal stability of these dielectrics on Si is a crucial issue by integrating them into CMOS, because standard device fabrication requires high temperature annealing, i.e. a dopant activation process (> 900 ^{o}C). The HfO_2 is one possible candidate because of its high dielectric constant and high conduction band offset. On the other hand the formation of metallic Hf-silicide or Hf-metal during the annealing process for activation is one of the most serious problems, because the electrical characteristics will be influenced drastically due to the leakage current through the metallic region. In this work we present a systematic electronic and structural study of the Hf-silicide formation upon annealing.

EXPERIMENT

The experiments were performed at DELTA (Accelerator Facility at the University Dortmund) using an undulator beam line with a photon energy of 200 eV and conventional MgKα radiation (1253.6 eV). The Si(111) crystal was cleaned in situ by resistive heating up to 1000 ^{o}C, resulting in a clean (7x7) reconstructed surface checked by LEED and XPS. A Hf wire tip heated by electron bombardment was used for depositing the 10 Å of the Hf films onto the Si(111) substrate at room temperature. The sample was annealed in consecutive steps of 1 hour for each one from room temperature to 960 ^{o}C (cf. figure 1). All XPS, LEED and XPD measurements were obtained with the sample at room temperature.

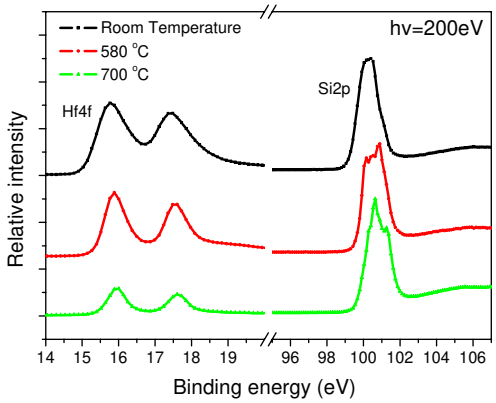

Figure 1 : Hf 4f (left) and Si 2p (right) XPS spectra obtained at room temperature (top), after annealing at 580 ^{o}C (medium) and after annealing at 700 ^{o}C (bottom)

In the angular XPD studies we used 200 eV (linear polarized synchrotron radiation) and 1253.6 eV (MgKα radiation).

RESULTS

By using the intensity ratio for the Hf 4f and Si 2p high-resolution photoelectron peaks as a function of annealing temperature we verified three phases during the heating (cf. figure 2b). After a heating of 500 °C the formation of HfSi occurred, after heating to 700 °C the Hf intensity decreases by diffusion. The first XPD measurements were carried out after heating to 580 °C in order to observe the initial phase during the formation of HfSi, the two further XPD patterns displayed in the second and third row were recorded after heating to 700 °C. The second and third rows were recorded of photon energies of 200 eV and 1253.6 eV, respectively. These preliminary results have to be compared to simulations in order to determine the structure.

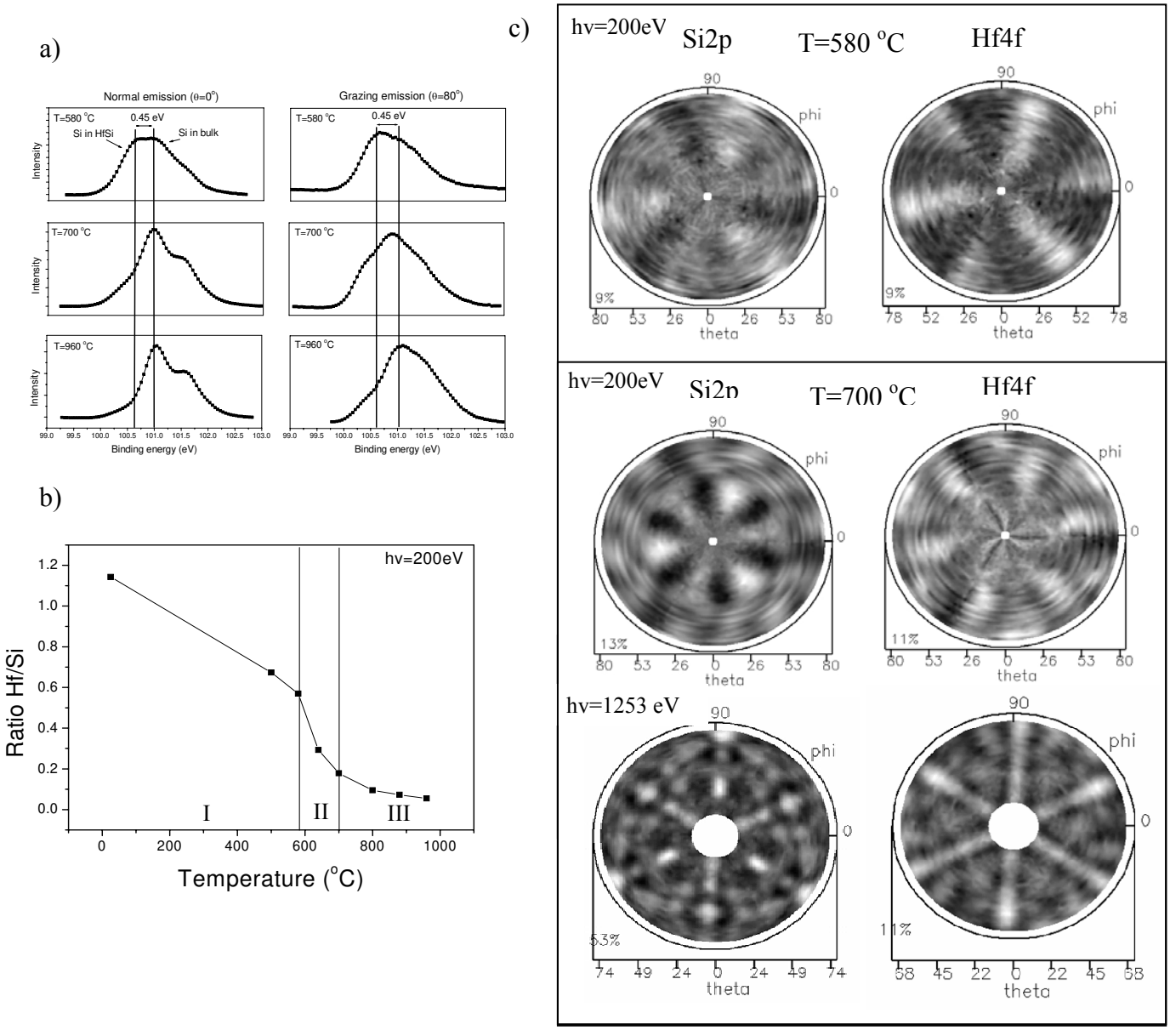

Figure 2 : (a) Si 2p high resolution XPS for different annealing temperatures, (b) intensity ratio of the Hf 4f and Si 2p in function of temperature and (c) photoelectron diffraction pattern for Si 2p and Hf 4f using photon energies of 200 eV at 580 °C (top) and 700 °C (medium) and using a photon energy of 1253.6 eV at 700 °C (bottom)

Structure determination of the system HfSi/Si(100) using XPS and XPD at beamline 11 at DELTA

C. Flüchter[1,*], D. Weier[1,2], S. Dreiner[1], M. Schürmann[1], U. Berges[1,2], M.F. Carazzolle[3], A. de Siervo[3,4], R. Landers[3,4], G.G. Kleiman[4], C. Westphal[1,2],

[1] Experimentelle Physik 1 - Universität Dortmund, Otto-Hahn-Str.4, D 44221 Dortmund, Germany
[2] DELTA - Universität Dortmund, Maria-Goeppert-Mayer-Str. 2, D 44227 Dortmund, Germany
[3] Laboratório Nacional de Luz Sincrotron, C.P. 6192, 13084-971 Campinas, SP, Brazil
[4] Instituto de Fisica - Universidade Estadual de Campinas, C.P. 6165, 13083-970 Campinas, SP, Brazil
[*] corresponding author: christian.fluechter@uni-dortmund.de

(November 2005)

Due to the continuing miniaturization of integrated circuits in the semiconductor industry, the insulating SiO_2 layer, one part of the layer stack used for example in MOSFETs (**M**etal **O**xide **S**emiconductor **F**ield **E**ffect **T**ransistor), will become obsolete in the near future. Rising leakage currents will make this material ineffective for use in transistors within the next two or three years. New compounds, so called *high-k* materials, are proposed [1] for replacement. One of the high-k candidates is hafnium oxide (HfO_2). We investigate a pre state of the system HfO_2/Si by determining the structure and electronics of the system HfSi/Si. This is done by X-ray photoelectron spectroscopy (XPS) and X-ray photoelectron diffraction (XPD). For the measurements high flux is needed in the soft X-ray regime , thus best results are obtained for synchrotron light as a exitation source.

The measurements were conducted at the new build up beamline 11 at DELTA. The primary energy for the experiment can precisely be selected by a plane grating monochromator (PGM) and is usually set to energies between 200 and 400 eV. The beam is collimated to a spotsize of $500\,\mu$m $\times$ $70\,\mu$m at the sample site. Ultrathin layers of hafnium (< 30 Å) are deposited onto the Si(100) sample by electron beam evaporation and a following heat treatment. High-resolution XPS spectra were obtained using a hemispherical analyzer and a set of nine electron channel detectors. XPD patterns were recorded by rotating the sample around two axis. All mechanical movements were carried out by a manipulator. An XPD pattern can be recorded automatically since all mechanical movements of the manipulator were carried out by stepping motors controlled by a computer program. The data aquisition time for one complete pattern is usually 20 to 40 hours, measuring the half space above the sample in steps of 2° in polar angle and 2° in azimuth angle.

Figure 1 shows a spectrum of the hafnuim 4f peak at a binding energy of around 15 eV. The sample was heated to 750°C for 10 minutes in order to obtain an ordered HfSi phase. The primary energy is $h\nu = 195$ eV. The observed doublet structure of the photoelectron signal is due to the spin-orbit splitting of 1.66 eV [2].

The inset of Figure 1 shows a diffraction pattern of the Hf 4f signal. Every point in the pattern represents the integrated photoelectron intensity of the Hf 4f peak at a certain angle. The intensity variations are caused by diffraction effects. In order to determine the atomic structure of the system at the interface a comparison the data to computer simulations for various structures has to be performed. The conducted simulations indicate that the systems

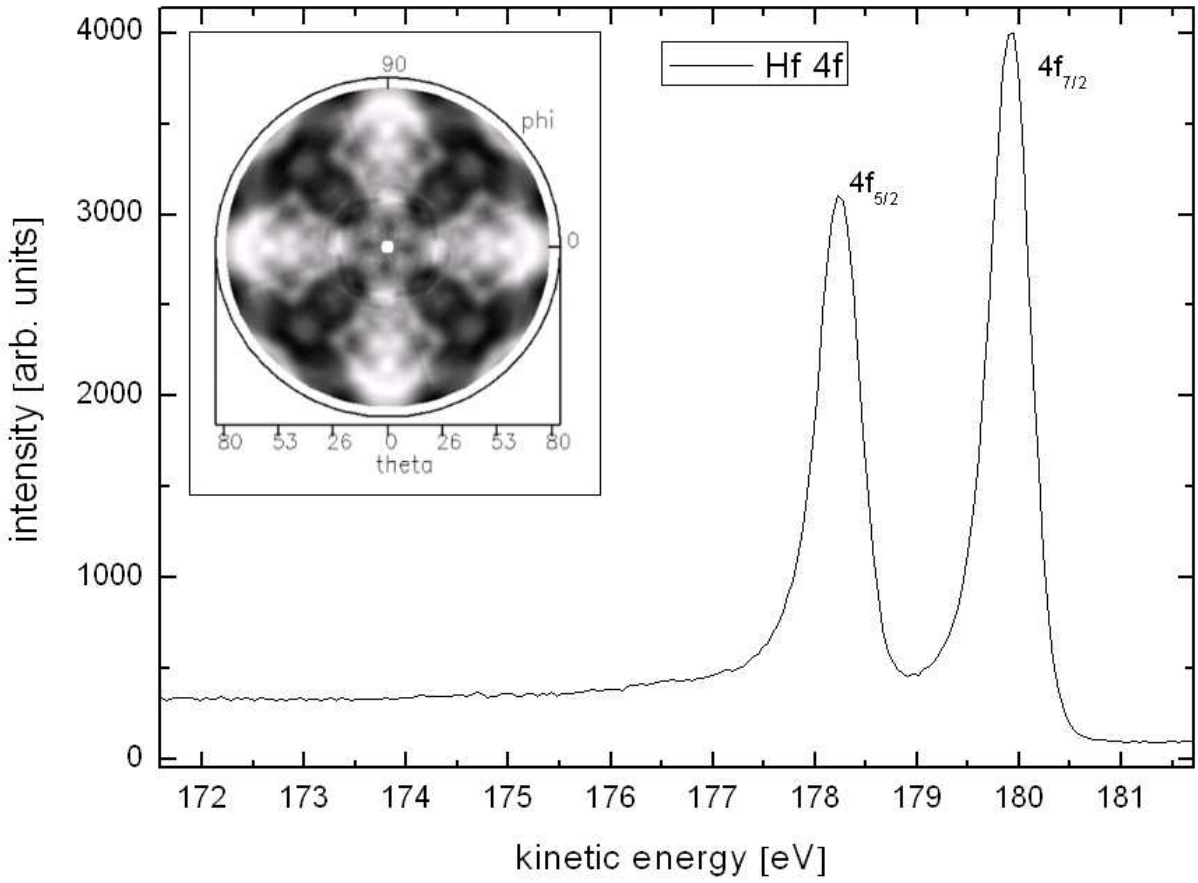

Figure 1: Spectrum of the hafnium 4f state in the hafnium/silicon compound. In respect to clean hafnium a chemical shift of 0.4 eV could be measured. Inset: Diffraction pattern of the Hf 4f signal in the half space above the sample ($E_{kin} = 160$ eV)

exists in a modification of the so called C49 or zirconium silicide structure. This structure was proposed for a bulk hafnium silicide crystal in 1957 [3]. The simulations are still in progress.

We investigated the structure of the system HfSi/Si(100) by means of photoelectron spectroscopy and photoelectron diffraction. It was possible to obtain an ordered hafnium silicide phase by heating the sample to temperatures above 600°C. Results from cumulative heating indicate a diffusion of hafnium into the silicon bulk. The obtained XPD diffraction patterns were compared to computer simulations. From this simulations we propose a modificated zirconium silicide structure for this system.

For further investigations we plan to oxidize the sample to obtain HfO_2-films. Another possibility would be to directly evaporate hafnium oxide onto the silicon wafer. Up to now nothing is known about the interface structure of hafnium oxide to silicon.

[1] G.D. Wilk, R.M. Wallace, J.M. Anthony, J. Appl. Phys., **89**, 5243 (2001)
[2] J. Kirz, D. Attwood, B. Henke, X-Ray Data Booklet, Lawrence Berkeley Laboratory (1986).
[3] J. F. Smith, D. M. Bailey, Acta Cryst. **10**, 341 (1957)

Photoelectron spectroscopy (XPS) and photoelectron diffraction (XPD) studies on the system hafnium oxide on Si(100)

D. Weier[1,2,*], C. Flüchter[1,2], A. de Siervo[3,4], M. Schürmann[1], S. Dreiner[1], U. Berges[1,2], M.F. Carazzolle[3], A. Pancotti[3], R. Landers[3,4], G.G. Kleiman[4], C. Westphal[1,2]

[1] Institut of Physics - University Dortmund, Otto-Hahn-Str.4, D 44221 Dortmund, Germany
[2] DELTA - University Dortmund, Maria-Goeppert-Mayer-Str. 2, D 44227 Dortmund, Germany
[3] Laboratório Nacional de Luz Sincrotron, C.P. 6192, 13084-971 Campinas, SP, Brazil
[4] Instituto de Fisica - Universidade Estadual de Campinas, C.P. 6165, 13083-970 Campinas, SP, Brazil
[*] corresponding author: daniel.weier@uni-dortmund.de

(October 2005)

Continuous down-scaling of silicon based MOSFETs results in device lengths of less than 100 nm. This requires a reduction of the gate dielectric thickness to less than 15 Å which is not possible for SiO_2 because of an increasing leakage current[1]. If thicker layers than 15 Å are grown then a high-k material with a less leakage current and with the same electrical properties as SiO_2 is obtained. Presently, there are many higk-k candidates discussed as a substitute for SiO_2 as the gate dielectric. One of the most promising candidates is HfO_2[2].

In our experiments ultra-thin films of HfO_2 on Si(100) were studied by XPD (X-ray Photoelectron Diffraction). A possible interface structure between silicon and hafnium oxide should become accessilbe as in the case of SiO_2[3]. The Si(100) surface is technologically very important because it is the most relevant surface in industrial manufacturing. Various different preparation recipes for hafnium oxide on Si(100) were investigated at the beamlines 5 and 11 of DELTA. These beamlines provide high flux and sufficient energy resolution in the soft x-ray range, for the planned XPS and XPD studies.

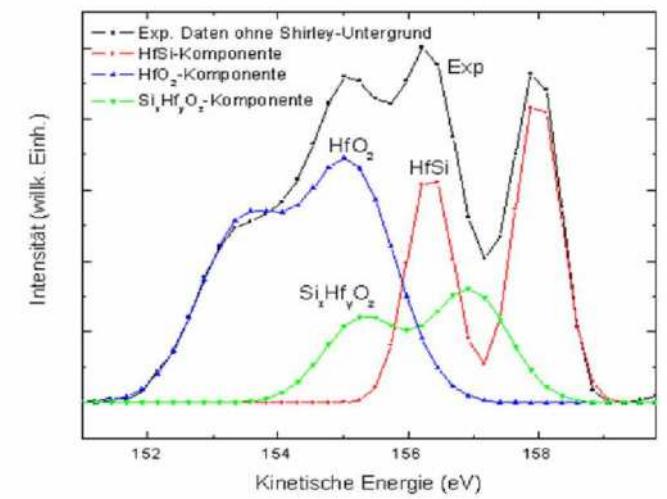

Figure 1: Hafnium 4f specta after substraction of a Shirley background (hv = 180 eV)

Sample preparation was started with the clean 2x1 reconstructed Si(100) surface. A small

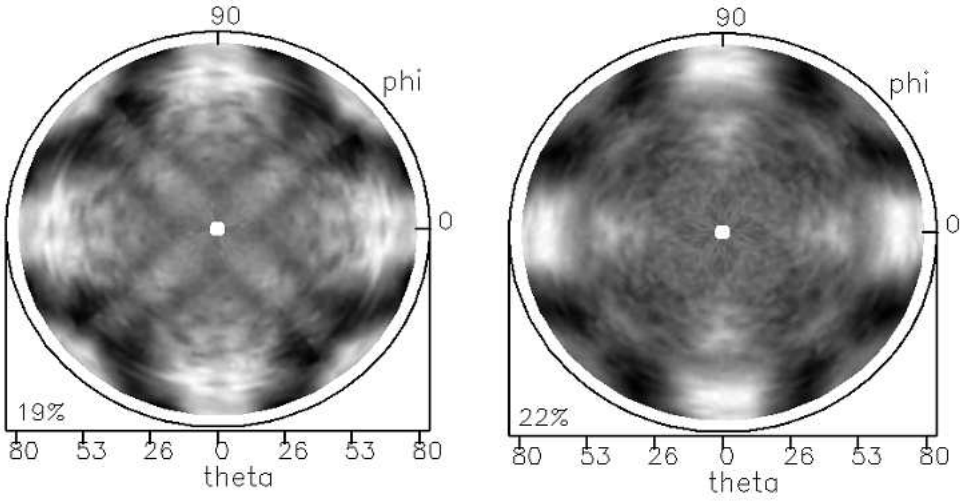

Figure 2: a.) Diffraction pattern of HfSi (E_{kin} = 158 eV, b.) Diffraction pattern of $Hf_xSi_yO_z$ (E_{kin} = 157 eV)

amount of hafnium was deposited onto the sample by electron beam evaporation to prevent the silicon from reacting to SiO_2 during the ongoing preparation. As the next step an oxygen partial pressure of $1{,}3{\cdot}10^{-8}$ mbar was provided in the chamber and the evaporation of hafnium was continued. The XPS spectrum of the resulting surface is shown in Figure 1. The Figure displays the components obtained by a least square fitting. The components belong to the three different oxidation states of hafnium on the sample. The spectrum shows that the surface contains of a combination of hafnium silicide and hafnium oxide. The peak width (full width at half maximum) of the hafnium oxide doublet signal is larger than the width of the silicate signal. This indicates that there are different components contained in the doublet. In order to separate the different components a fitting procedure was apllied to the spectrum. As a result, three individual components of the spectrum were obtained. Figure 1 displays the components of hafnium dioxide (HfO_2), hafnium silicate ($Hf_xSi_yO_z$), and hafnium silicide ($HfSi_2$) at binding energies of 154.4 eV, 157 eV, and 158 eV, respectively. The corresponding diffraction patterns of the $HfSi_2$ and the $Hf_xSi_yO_z$ are displayed in Figure 2.

The component of the HfO_2-signal shows no diffraction features indicating an amorphous phase of hafnium oxide without any short range order. The signal of the $HfSi_2$ component displays a diffraction pattern which is similar to a diffraction pattern, which was obtained in a previous study by our group at DELTA for a thick hafnium silicide film on Si(100). A possible interpretation could be that there are areas on the sample which consist of a thick ordered layer of hafnium silicide. The signal of the $Hf_xSi_yO_z$ component displays a diffraction pattern which indicates ordered hafnium silicate on the sample. The two diffraction patterns are different, reflecting their individual atomic environment. Presently, the experimental diffraction patterns are compared to calculated patterns for models of the interface between hafnium oxide and crystalline silicon.

[1] J.H. Stathis and D.J. DiMaria, Tech. Dig. Int. Electron Devices Meet. 1998, 167
[2] G.D. Wilk, R.M. Wallace and J.M. Anthony, J. Appl. Phys. **89**, 5243 (2001)
[3] S. Dreiner, M. Schürmann, C. Westphal, Physical Review Letters **93**, 126101 (2004)

STATUS OF THE VUV-BEAMLINES U55 (BL11) AND TGM3 (BL12) AT DELTA

Ulf Berges, Swen Doering and Carsten Westphal

DELTA, University of Dortmund, Maria-Goeppert-Mayer Str. 2, Dortmund, Germany
Experimental Physics I, University of Dortmund, Otto-Hahn-Str. 4, Dortmund, Germany

The beamlines U55 (BL 11) and TGM3 (BL 12) in the VUV-range at the storage ring facility DELTA are set up and operated by the group Experimental Physics Ib at the department of Physics of the university of Dortmund. First experiments are performed at the U55-Beamline by this group to gain experience with this beamline. The TGM3-Beamline is still under commissioning.

U55-BEAMLINE

The U55-Beamline is working in the energy range between 55 and 1500 eV. The linearly polarized synchrotron radiation is generated by a permanent magnet undulator with a variable gap between 20 and 200 mm as insertion device. The beamline uses a PGM-setup with two gratings (400 and 1200 lines/mm) and a variable exit slit up to 3 mm. The designed photon flux is 10^{10} to 10^{11} photons/s/0.1A @20 µm Exit slit and 10^{12} to 10^{13} photons/s/0.1A @200 µm. The designed energy resolution is up to 30000 @ 20 µm and between 1000 and 8000 @ 100 µm. The expected focus size at the experiment is 70 x 30 μm^2. The planned experiments are photoemission spectroscopy (XPS) and photoelectron diffraction pattern (XPD) of the interface layer of semiconductors.

At the beginning of this year the reliability of the beamline has been increased by the mounting of additional encoders to measure the real position of the most beamline motors. None mayor failure occurs during beamtime. The photodiode after the exit slit used for flux measurements and beamline optimization has to be replaced. The beamline optimization program can still be continued due to a second photodiode behind the last focusing mirror of the beamline. The measured photon flux at this diode is about 10^{12} photons/s/100mA @ 200 µm exit slits. The flux at small exit slits has still to be increased by a factor 20 to achieve design values due to the not completely optimized settings of the beamline elements. The energy resolution has been tested at 400 eV with nitrogen and has to be improved.

The monochromator was tested with beam during the first synchrotron radiation runs of this year. First beam at the experiment was achieved on the end of April. During the following synchrotron radiation weeks of DELTA various XPS and XPD experiments at different probes with the experimental chamber of the group have been performed at different beamline energies between 200 and 800 eV (see four reports of Schürmann, Flüchter, Weier and Carazzolle). In

between the beamline setup has been improved to achieve a higher photon flux and energy resolution. The actual beamline setup is sufficient for the performed measurements, but still has to be improved for the planned experiments during the next year (photon flux at small exit slits and energy resolution).

TGM3-BEAMLINE

The TGM3-Beamline is a dipole beamline in the energy range between 6 and 200 eV. Planned experiments are photoelectron spectroscopy in the valence band regime and Fermisurface-Mapping. The former BESSYI-beamline has been adapted to the situation at DELTA. The expected photon flux is in the order of the old BESSYI-setup. The optical layout was kept, the vacuum system and diagnostics improved. The beamline is completely build up. During this year the monochromator motor has been integrated into the new beamline control system at DELTA to allow an easier adjustment of the three under vacuum interchangeable gratings. The beamline consists of the focusing mirror, entrance slit, monochromator, exit slit and refocusing mirror. Synchrotron radiation has reached the monochromator. Stability measurements concerning the first focusing mirror have been performed. Due to the insufficient motorization and missing water cooling of this mirror a beamline optimization and stable operation is difficult. So a new chamber for the first mirror has been designed to improve the beamline setup and will be ordered in near future. A gas cell and photodiode to perform first measurements with beam at the experiment have been integrated into the beamline. The expected photon flux at the experiment is in the order of 10^{11} photons/s/100mA between 30 and 80 eV with the 600 lines/mm grating and 10^{10} photons/s/100mA between 80 and 200 eV with the 1800 lines/mm grating. The beam size at the source point at DELTA is 136 x 65 μm^2, the divergence 194 x 9 μrad^2. The beam size at BESSYI was three times bigger, the divergence in the same order. The smaller beam size and the higher electron beam energy at DELTA lead to an increased heat load on the first mirror. This is a reason for the observed stability problems at the first mirror.